

# Colloidal Nanoparticles of High Entropy Materials: Capabilities, Challenges, and Opportunities in Synthesis and Characterization

Gaurav R. Dey, Samuel S. Soliman, Connor R. McCormick, Charles H. Wood, Rowan R. Katzbaer, and Raymond E. Schaak\*



Cite This: *ACS Nanosci. Au* 2024, 4, 3–20



Read Online

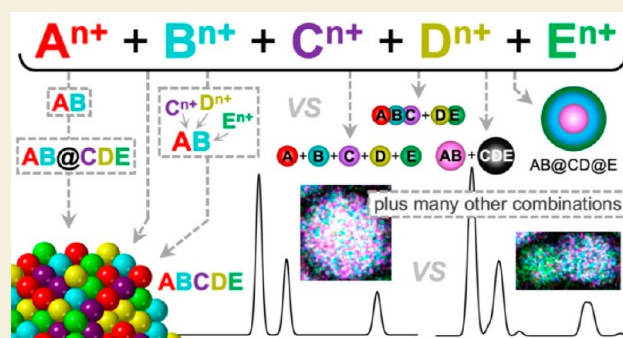
ACCESS |

 Metrics & More

 Article Recommendations

**ABSTRACT:** Materials referred to as “high entropy” contain a large number of elements randomly distributed on the lattice sites of a crystalline solid, such that a high configurational entropy is presumed to contribute significantly to their formation and stability. High temperatures are typically required to achieve entropy stabilization, which can make it challenging to synthesize colloidal nanoparticles of high entropy materials. Nonetheless, strategies are emerging for the synthesis of colloidal high entropy nanoparticles, which are of interest for their synergistic properties and unique catalytic functions that arise from the large number of constituent elements and their interactions. In this Perspective, we highlight the classes of materials that have been made as colloidal high entropy nanoparticles as well as insights into the synthetic methods and the pathways by which they form. We then discuss the concept of “high entropy” within the context of colloidal materials synthesized at much lower temperatures than are typically required for entropy to drive their formation. Next, we identify and address challenges and opportunities in the field of high entropy nanoparticle synthesis. We emphasize aspects of materials characterization that are especially important to consider for nanoparticles of high entropy materials, including powder X-ray diffraction and elemental mapping with scanning transmission electron microscopy, which are among the most commonly used techniques in laboratory settings. Finally, we share perspectives on emerging opportunities and future directions involving colloidal nanoparticles of high entropy materials, with an emphasis on synthesis, characterization, and fundamental knowledge that is needed for anticipated advances in key application areas.

**KEYWORDS:** *high entropy alloys, high entropy materials, nanoparticles, nanocrystals, complex solid solutions, nanochemistry*



The term “high entropy” has become a buzzword in the world of nanoparticles. “High entropy” often refers to the entropic driving force by which alloys and solid solutions that generally have five or more principal elements in near-equal ratios are presumed to form.<sup>1</sup> In such materials, a high configurational entropy, due to the randomization of so many elements among equivalent lattice sites of a crystalline solid, wins out over the enthalpic penalty that comes from mixing them. More quantitatively, if the  $T\Delta S$  term of the Gibbs free energy equation ( $\Delta G = \Delta H - T\Delta S$ ) is sufficiently large, a “high entropy” material can form.<sup>1</sup> Mixing a large number of elements in a crystalline solid can satisfy this criterion, making  $\Delta G$  negative and allowing an alloy or solid solution to form, even if the enthalpy term ( $\Delta H$ ) is positive.<sup>1</sup> However, the “high entropy” classification with regard to solution-synthesized (colloidal) nanoparticles often refers more to the composition than to thermodynamic aspects of their formation.<sup>2–4</sup> With these considerations in mind, the past few years have seen a rapid rise in reports describing the

synthesis of colloidal nanoparticles of “high entropy” materials that contain five or more principal elements.

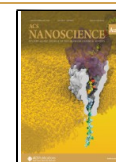
In this Perspective, we share some of the motivations, both fundamental and applied, that are catapulting this field to “buzzword” status. We briefly describe how nanoparticles of high entropy materials are made and then highlight the most common classes of colloidal high entropy nanoparticles. Next, we provide emerging insights, based on very recent studies, into the pathways by which colloidal high entropy nanoparticles form, along with the implications of these pathways on key nanoparticle features. We then discuss the meaning of the term “high entropy” in the context of the pathways by

**Received:** September 24, 2023

**Revised:** October 26, 2023

**Accepted:** October 26, 2023

**Published:** November 16, 2023



which so-called colloidal high entropy nanoparticles form. Finally, we identify and address challenges and opportunities in the field of high entropy nanoparticle synthesis. Among the most important challenges are in the characterization of colloidal high entropy nanoparticles, as the mainstream techniques that are most readily available must be used carefully due to the unique attributes of these compositionally complex nanoscale materials. Additional challenges include heterogeneities within and among particles, identifying and understanding nanoparticle formation pathways, dealing with complex and competing chemical reactivities during synthesis, and characterizing bulk and surface composition and structure. We then offer perspectives on emerging and future opportunities of high entropy nanoparticles.

### ■ WHY DO RESEARCHERS CARE ABOUT NANOPARTICLES OF HIGH ENTROPY MATERIALS?

Ever since the introduction of bulk high entropy alloys<sup>1,5</sup> and bulk high entropy oxides,<sup>6</sup> it was recognized that the randomization of a large number of elements within a crystalline solid leads to unique properties not exhibited by the end members. The so-called “cocktail effect” colloquially describes the functional benefits arising from the synergistic interactions among the many randomized elements.<sup>7</sup> This cocktail effect, coupled with the high surface-to-volume ratio that is associated with nanoparticles, has led to significant interest in high entropy nanoparticles for applications in heterogeneous catalysis.<sup>3,8</sup> Here, gas-phase and liquid-phase catalytic reactions occur at active sites on the surface of a solid. These active sites are atomic arrangements with precise structures and chemical features that offer optimal binding energies to carry out catalytic transformations effectively and efficiently.<sup>3,8</sup> As the size of a nanoparticle decreases, the surface area and, concomitantly, the number of active sites per unit of overall material (mass, volume, etc.) increase. The cocktail effect results in unique active sites with catalytic capabilities that are not possible in compositionally simpler materials as well as localized lattice distortions that enhance catalytic activity and sluggish diffusion (of the atoms in the high entropy alloy crystal structure) that improves catalytic durability.<sup>3,8</sup> Coupling this cocktail effect with high active site densities makes nanoparticles of high entropy materials important and practical and therefore motivates their synthesis.

### ■ HOW DO WE MAKE NANOPARTICLES OF HIGH ENTROPY MATERIALS?

If the primary *thermodynamic* driving force for forming high entropy materials is a large magnitude of the  $T\Delta S$  term in the Gibbs free energy equation, then high temperatures during synthesis are an important complement to the high configurational entropy that comes from the composition. However, high temperatures favor the growth and sintering of a material, which increases the sizes of the grains that constitute it. Therefore, high temperatures generally disfavor the formation of nanoparticles. Bulk synthesis methods for high entropy materials also often involve rapid quenching from the high temperatures at which they form. Quenching helps to trap the system in the phase it is in at high temperatures, preventing it from equilibrating at intermediate temperatures (where the high entropy phase is no longer favored) during cooling. For these reasons, the earliest methods for synthesizing nano-

particles of high entropy materials involved rapid heating of bulk reagents to very high temperatures followed by rapid cooling to trap the entropy-stabilized phase. These methods used techniques such as mechanical alloying,<sup>9</sup> sputtering deposition,<sup>10,11</sup> laser ablation,<sup>12</sup> ultrasonication,<sup>13</sup> spray pyrolysis,<sup>14,15</sup> microwave heating,<sup>16</sup> and even subjecting the sample to thermal “shocks”.<sup>2</sup>

Given these considerations of rapid heating and rapid cooling, a team of researchers in 2018 showed that metal salts loaded onto refractory (thermally stable) catalytic supports could be rapidly heated to temperatures of  $\sim 2000$  K within  $\sim 55$  ms to facilitate reduction and mixing, forming a high entropy phase.<sup>2</sup> Cooling at an equally rapid rate trapped the high-temperature high entropy phase and allowed it to persist at room temperature.<sup>2</sup> By anchoring the metal salts to a high surface area support, particles formed instead of bulk materials, and growth and sintering were minimized because of particle-support interactions. Additionally, the high-temperature dwell time was minimal, which also prevented growth and sintering. This carbothermal shock method has produced nanoparticles of high entropy alloys containing up to 15 different metals,<sup>17</sup> high entropy intermetallics containing up to eight metals,<sup>18</sup> and high entropy oxides containing up to 10 elements.<sup>19</sup> Following the development of this approach, other established methods offering complementary features were applied to high entropy materials with increasing frequency. These methods include spray pyrolysis,<sup>14,15</sup> sputtering deposition,<sup>10,11</sup> kinetically controlled laser synthesis,<sup>12</sup> solution combustion,<sup>20</sup> and ultrasonication-assisted wet chemistry.<sup>13</sup> In general, these techniques tend to require sophisticated setups and/or equipment and sometimes lack scalability, preventing the production of large quantities of material. Additionally, these methods limit control over composition and morphology, which are important for nanoparticle materials, especially for applications in catalysis, where particle shape can influence catalytic mechanisms, products, and product distributions.

Solution methods are among the most widely used synthetic platforms for making nanoparticles, as they have been proven to be capable of rigorously controlling size and shape across a wide range of diverse materials while also yielding isolatable quantities of material and, in some cases, being scalable.<sup>21–25</sup> Here, appropriate reagents, including salts and/or complexes, are dissolved in a solvent in which they are soluble and then thermally and/or chemically triggered to react, which initiates particle nucleation. Then, in the presence of ligands, surfactants, coordinating solvents, and/or counterions, growth occurs under conditions that maintain nanoscale dimensions while favoring and disfavoring certain crystal facets to allow different shapes to evolve. Much is known, and even more continues to be learned, about how various types of colloidal nanoparticles form and grow in solution. High entropy materials, which generally contain five or more elements in nearly equal proportions, represent a challenging extension of colloidal nanoparticle synthetic chemistry. For example, in the synthesis of colloidal high entropy alloy nanoparticles, each metal reagent will have its own reactivity profile, including different reaction rates and threshold reaction temperatures, that defines how and when it will reduce, decompose, dissociate, coordinate, nucleate, and diffuse as well as how long it will take to do so. In some cases, there can be competitive reactivities, whereby one reagent in the presence of others can behave differently. For example, a metal salt that would normally reduce, nucleate, and grow a metal nano-

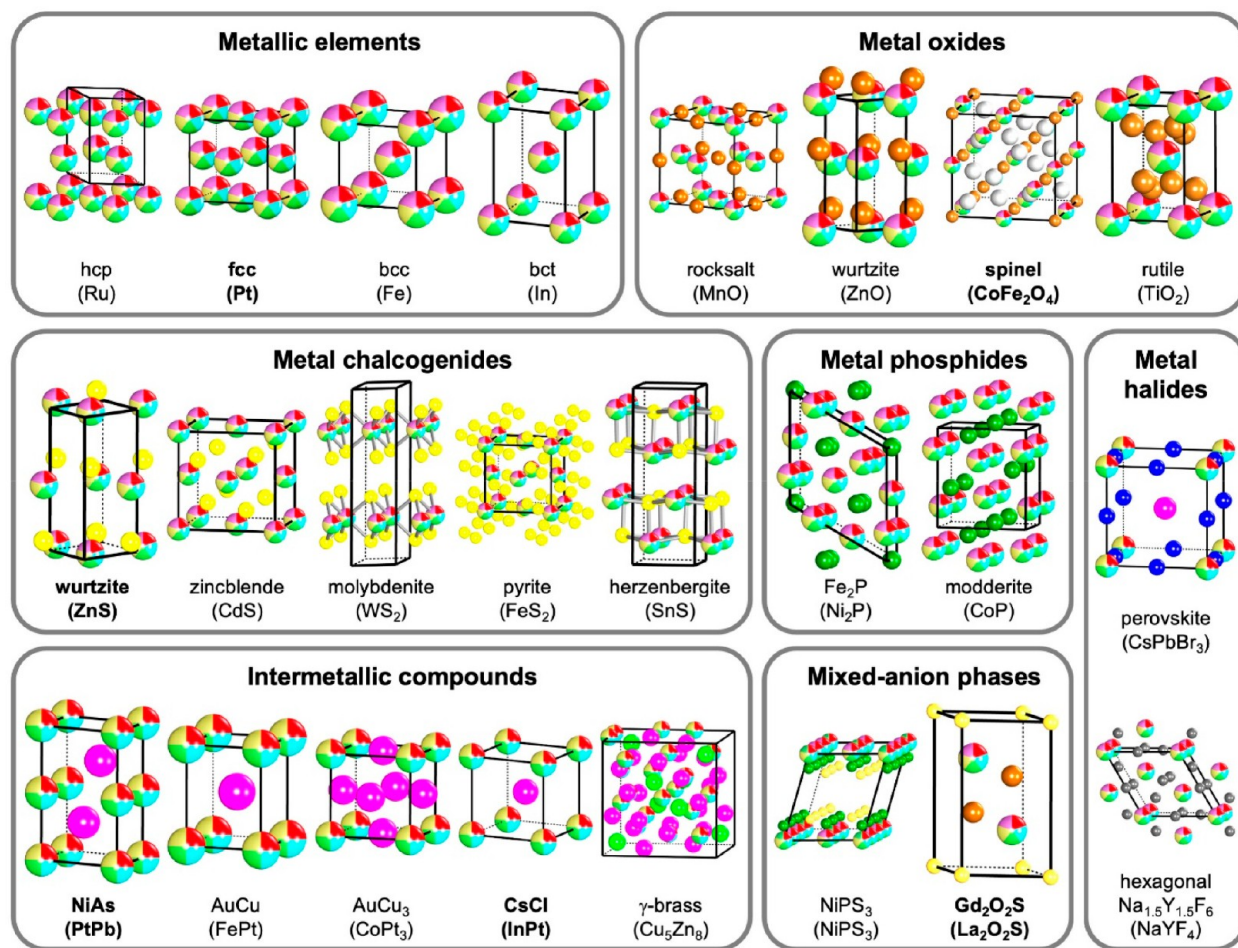


**Figure 1.** Crystal structures, along with example compositions, of some of the materials that are most commonly synthesized as colloidal nanocrystals. All are shown as high-entropy variants, with the randomized site(s) indicated with multicolored atoms. Those that are bolded have been successfully synthesized as colloidal nanocrystals; others may be possible in the future.

particle under a certain set of conditions could instead undergo galvanic replacement (either before or after reducing) in the presence of a different metal salt. These issues complicate the synthesis of colloidal high entropy materials, which are the focus of this Perspective. Despite these challenges, significant progress has been made, and capabilities are quickly emerging and expanding.

### ■ WHAT TYPES OF COLLOIDAL HIGH ENTROPY NANOPARTICLES HAVE BEEN MADE?

The high entropy materials that have been synthesized and studied the most as colloidal nanoparticles are metal alloys,<sup>26,27</sup> due in large part to their desirable catalytic properties. Other classes of colloidal high entropy nanoparticles that have been reported include intermetallic compounds,<sup>28–31</sup> metal sulfides,<sup>32–37</sup> metal oxides,<sup>38–41</sup> and metal oxysulfides.<sup>42</sup> Progress is also being made toward accessing additional types of colloidal high entropy nanoparticles. Figure 1 provides an overview of some crystal structures that are known to be synthetically accessible as colloidal nanoparticles, adapted to show them as high entropy phases and highlighting (in bold) some of those that have been synthesized to date.

#### Colloidal High Entropy Alloy Nanoparticles

Several common variants of the general synthetic platform for making colloidal metal nanoparticles described above have

been applied to the formation of high entropy alloy nanoparticles, often enabled by kinetic rather than thermodynamic control. One of the most common methods involves simultaneously adding a solution containing a mixture of all metal reagents to a heated solvent, which may also serve as a reducing agent.<sup>26,27</sup> Implementing this approach with dropwise addition of the salt solution mixture into the heated solvent can allow for careful control over the reaction kinetics. Alternatively, the appropriate metal salts, reducing agents, and solvents can be combined together at room temperature and then heated to the final reaction temperature.<sup>43,44</sup> An emerging approach is to synthesize colloidal core–shell nanoparticles with different compositions and then subsequently anneal them to facilitate diffusion and mixing, which transforms them to high entropy alloys.<sup>45–47</sup> These methods differ from one another in aspects of their reagents and reaction conditions, including choice of salts, solvents, reducing agents, reaction temperatures, and reaction times. However, they all use well-established colloidal synthetic techniques that are minor variations of mainstream methods, which makes them straightforward to implement.

Using these methods, colloidal high entropy alloy nanoparticles containing between five and eight metals have been made. Of these, most contain exclusively or predominantly platinum group metals, such as RuRhPdOsIrPt,<sup>26</sup> as these are the easiest to reduce from metal salts to zero-valent metals and

their reduction generally occurs rapidly. A few reports have convincingly incorporated nonprecious metals into colloidal high entropy alloy nanoparticles using similar methods, including NiFeCoPdPt<sup>27</sup> and PtNiFeCoCu.<sup>44</sup> However, the more dissimilar the constituent elements and their reactivities are, the more likely that phase segregation may win out over the homogeneous incorporation of all elements within the nanoparticle. It is possible to sidestep this challenge of concurrent reduction and mixing by using seed-mediated coreduction to synthesize uniform nanocrystals with compositional segregation. For example, Pt, Ni, and Co coreduce on presynthesized PdCu nanoparticles; the resulting colloidal PtNiCo@PdCu core–shell nanoparticles can be deposited onto a refractory support and annealed at higher temperatures to transform them into PdCuPtNiCo high entropy alloy nanoparticles with retention of size and morphology.<sup>45</sup> While the products are no longer colloidal, the use of colloidal precursors has the potential to capture the best capabilities from both the colloidal nanoparticle synthesis and the high-temperature heating approaches.

### Colloidal High Entropy Intermetallic Nanoparticles

In crystalline alloys, all elements are presumed to be randomly distributed among the lattice sites of simple crystal structures based on those of the elements, which most commonly include primitive cubic, body-centered cubic (bcc), hexagonal close-packed (hcp), and cubic close-packed (ccp), which is the same as face-centered cubic (fcc). Intermetallic compounds, in contrast, are defined by their crystallographic ordering. Different elements are on different lattice sites, and this ordering imparts unique properties, including in catalysis. For example, as is now well-established among two-metal ordered intermetallics, elements on one site can facilitate catalysis while others on a different site prevent poisoning.<sup>48,49</sup> For example, the crystal structures of elemental Pt and elemental Pb are both fcc, but a 1:1 PtPb alloy adopts the NiAs crystal structure, which has an hcp arrangement of Pb atoms with Pt occupying the octahedral interstitial sites. High entropy intermetallic nanoparticles remain rare.  $L1_0$ -type Pt(Fe<sub>0.7</sub>Co<sub>0.1</sub>Ni<sub>0.1</sub>Cu<sub>0.1</sub>) and (Pt<sub>0.8</sub>Pd<sub>0.1</sub>Au<sub>0.1</sub>)(Fe<sub>0.6</sub>Co<sub>0.1</sub>Ni<sub>0.1</sub>Cu<sub>0.1</sub>Sn<sub>0.1</sub>) intermetallic nanoparticles were made by carbothermal shock, first forming alloys that transformed to intermetallics upon reheating to ~1100 K for 5 min and then rapidly quenching.<sup>18</sup> Colloidal high entropy intermetallic nanoparticles made directly in solution include NiAs-type PtRhBiSnSb<sup>28</sup> and PtBiPb@PtBiNiCo core@shell nanoplates<sup>30</sup> via thermal decomposition of the corresponding metal reagents and Ni<sub>2</sub>In-type (Pd, Rh, Ir, Pt)Sn via a slow injection method.<sup>29</sup> In this latter example, comparison of the key compositional, structural, and morphological features of the (Pd, Rh, Ir, Pt)Sn nanoparticles with those of their 14 constituent binary, ternary, and quaternary variants shows how the synthetic evolution of the (Pd, Rh, Ir, Pt)Sn nanoparticles relates in a predictable way to the simpler systems.<sup>29</sup>

### Colloidal High Entropy Chalcogenide and Phosphide Nanoparticles

Solvothermal methods have been reported to produce a limited number of high entropy metal sulfide nanoparticles,<sup>33–36</sup> but to our knowledge, high entropy metal selenide and telluride nanoparticles have not yet been reported using colloidal synthesis techniques. Similarly, colloidal high entropy metal phosphide nanoparticles have not yet been reported, although progress has been made in targeting three-

metal colloidal phosphide nanoparticles.<sup>50</sup> In general, high entropy chalcogenide and phosphide nanoparticles have been slower to emerge than alloy systems, despite the frequency with which single-metal chalcogenide and phosphide colloidal nanoparticles are synthesized. To make metal sulfide and phosphide nanoparticles, one must react metal salts and/or complexes with chalcogen or phosphide reagents. These reagents have the chalcogen or phosphorus atoms bound within a stable molecule, such as dodecanethiol for sulfides or trioctylphosphine for phosphides. Temperatures of several hundred degrees Celsius are often needed to decompose these reagents and generate the reactive chalcogen or phosphorus species in solution, which then must react with the solubilized metal reagents. This process has more complex reaction chemistry and is therefore potentially more difficult to understand and control than for alloys. To sidestep this challenge for metal sulfides, cation exchange can be used to separate formation of a crystalline metal sulfide from incorporation and randomization of five cations.<sup>32</sup> For example, the Cu<sup>+</sup> cations in nanoparticles of roxbyite copper sulfide, which has a distorted hcp sulfur structure, can undergo simultaneous partial exchange with Zn<sup>2+</sup>, Co<sup>2+</sup>, In<sup>3+</sup>, and Ga<sup>3+</sup> to form the high entropy sulfide (Zn, Co, Cu, In, Ga)S, which adopts a wurtzite crystal structure that represents the idealized nondistorted structure of roxbyite.<sup>32</sup>

### Colloidal High Entropy Oxide Nanoparticles

Like the chalcogenides and phosphides described above, colloidal high entropy oxide nanoparticles remain rare, and the considerations and techniques for synthesis differ from other classes of compounds. Unlike for chalcogenides and phosphides, there is no standard molecular reagent that decomposes to release oxide anions in solution that can react to form oxides. Rather, the oxygen in oxides is often incorporated through reagents and solvents containing –OH or –OR groups.<sup>51</sup> As a result, the synthesis of colloidal oxide nanoparticles is often approached differently than the previously mentioned classes of materials. A common approach involves thermal or catalyzed decomposition in solution of a complex that has a metal directly bonded to oxygen, such as metal alkoxides, oleates, or stearates, and/or the use of mild pressure in solvothermal reactors. For example, (Co, Cu, Fe, Mn, Ni)<sub>3</sub>O<sub>4</sub> spinel nanoparticles were synthesized by first solvothermally reacting acetate salts of the corresponding metals mixed with ethanol, ethylene glycol, various surfactants, and hexamethylenetetramine, followed by heating at 400 °C to pyrolyze the organics and crystallize the product. These annealing steps render the particles noncolloidal, but the product formed after pyrolysis remains nanoscopic, albeit agglomerated.<sup>40</sup> A polyol reaction, using ethylene glycol as a complexing agent and sodium hydroxide as a source of OH<sup>–</sup>, yielded nanosheets of a high entropy hydroxide containing Cr, Mn, Fe, Co, Ni, and Zn. The high entropy perovskites Ba(FeNbTiZrTa)O<sub>3</sub>, Ba(MnNbTiZrTa)O<sub>3</sub>, Ba(FeSnTiZrTa)O<sub>3</sub>, and Ba(FeVTiZrTa)O<sub>3</sub>, were made solvothermally as nanoparticulate powders using an ionic liquid.<sup>38</sup> As is clear from these descriptions, high entropy nanoparticulate oxides can be synthesized using solution-based methods, but truly colloidal high entropy oxide nanoparticles of high crystalline quality are not usually produced.

### Other Classes of Colloidal High Entropy Nanoparticles

The scope of synthetically accessible colloidal nanoparticles is far more diverse than the few classes noted above, and indeed,

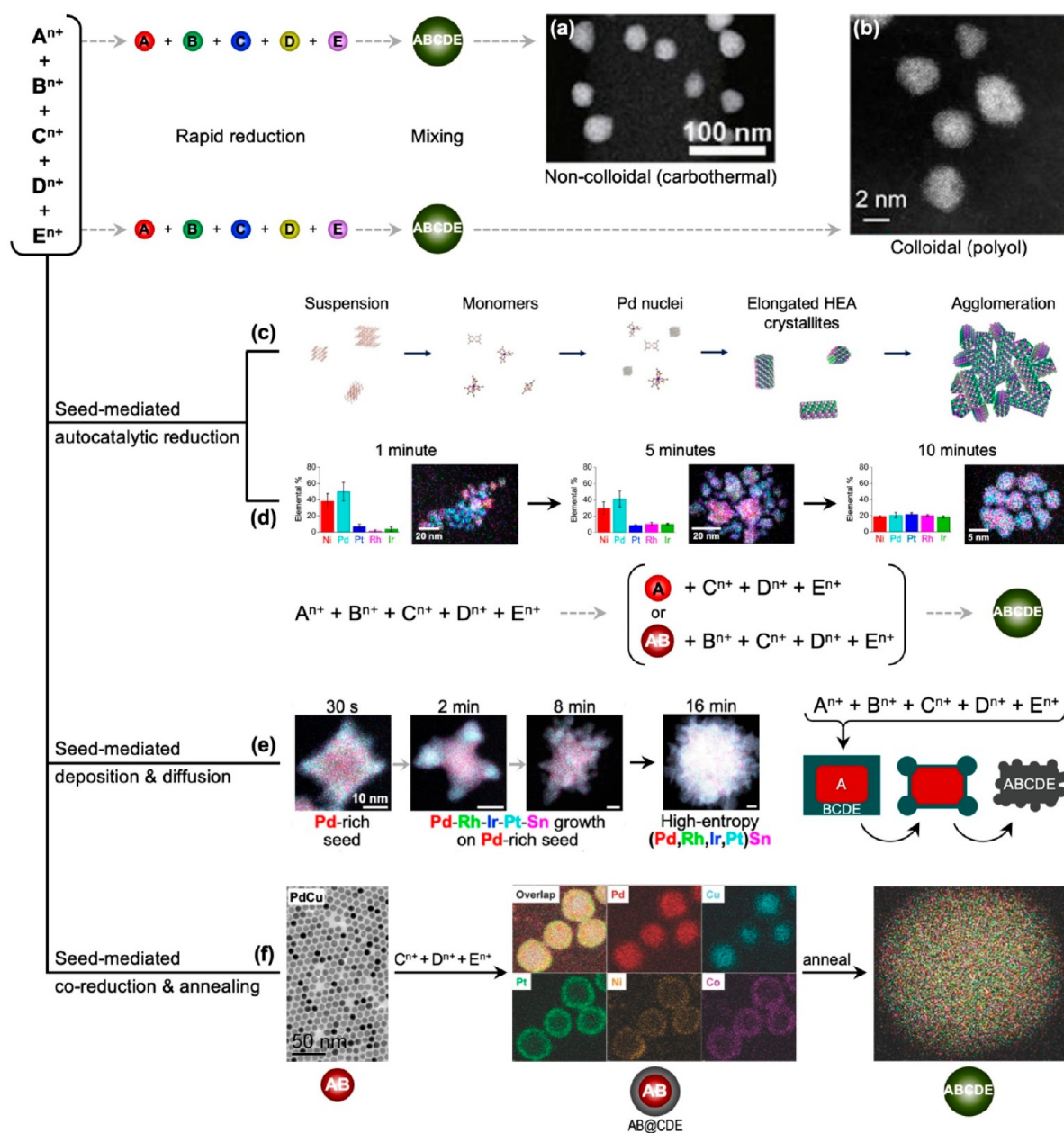


**Figure 2.** Brief overview of the primary types of pathways that have been identified in the formation of colloidal high entropy nanoparticles from reactions starting from five metal salts ( $A^{n+}$ ,  $B^{n+}$ ,  $C^{n+}$ ,  $D^{n+}$ , and  $E^{n+}$ ). Putative reaction pathways involving direct reduction and mixing are shown across the top. Reactions involving multistep pathways, which have been investigated and identified experimentally, are also shown. Examples include seed-mediated autocatalytic reduction, seed-mediated deposition and diffusion, and seed-mediated coreduction and annealing. Panel (a) is reproduced with permission from ref 2. Copyright 2018 the authors of ref 2, exclusive licensee American Association for the Advancement of Science. Panel (b) is reproduced from ref 26. Copyright 2020 American Chemical Society. Panel (c) is reproduced with permission from ref 43. Copyright 2020 Wiley-VCH. Panel (d) is adapted from ref 27. Copyright 2023 American Chemical Society. Panel (e) is adapted from ref 29. Copyright 2023 American Chemical Society. Panel (f) is adapted with permission from ref 45. Copyright 2021 Royal Society of Chemistry.

efforts to synthesize high entropy variants of a broader class of materials are underway. As one example that merges the preceding oxide and chalcogenide sections, the high entropy lanthanide oxysulfide  $\text{Ln}_2\text{O}_2\text{S}$  was recently synthesized as colloidal nanocrystals by thermally decomposing diethyl dithiocarbamates of Pr, Nd, Gd, Dy, and Er simultaneously in the presence of oleylamine, octadecene, and oleic acid, which serve as solvents and surface stabilizers.<sup>42</sup> These lanthanide oxysulfides are layered compounds that interleave planes of sulfur with staggered double layers of lanthanide oxide.

## HOW DO COLLOIDAL HIGH ENTROPY NANOPARTICLES FORM AND GROW?

Figure 2 presents a brief overview of pathways used to synthesize colloidal nanoparticles of high entropy materials. In many of the earliest reports of colloidal high entropy nanoparticles, the focus was on making new compositions, and for good reason. However, less emphasis was placed on how exactly they form, despite the complex and fundamentally interesting chemistry that undoubtedly must be occurring during the reactions that produce them. An early assumption

was that all the reagents coreact at the same time, such that all metals combine simultaneously and homogeneously in the growing nanoparticle.<sup>26</sup> However, it is becoming clear that this is not necessarily the case, at least not universally. During a solvothermal synthesis of PtIrPdRhRu nanoparticles, the formation of a Pd seed was found to occur first, followed by autocatalytic reduction of the other metals onto the (111) facets of the growing crystallite.<sup>43</sup> This same study, which represented an important milestone in understanding chemical details of reactions that lead to the formation of colloidal high entropy alloy nanoparticles, identified the importance of reagents and solvents as well as the reaction temperature and time in forming systems that were alloyed versus phase-segregated. Overall, it was found that the reaction pathway was driven by reduction kinetics and the relative rates of reaction and not by the assumed thermodynamic “boost” of a large  $T\Delta S$  term.<sup>43</sup>

The study highlighted above used an experimental setup that differed from the mainstream ones that are most common in colloidal nanoparticle synthesis, so that *in situ* data could be acquired. A similar pathway was identified during the colloidal synthesis of NiPdPtRhIr and related nanoparticles.<sup>27</sup> This reaction setup, involving the slow simultaneous injection of dissolved metal salts into a heated solvent mixture, is common in metal and alloy nanoparticle synthesis and as a result produces colloidally stable nanoparticles with diameters of approximately 10 nm. In this reaction, a Pd-rich NiPd seed formed first, followed by incorporation of the other elements. Early in the reaction, an initial rapid increase in the amount of Pd, at the expense of Ni, was observed, followed by an autocatalytic process whereby the other metals were reduced, deposited, and incorporated into the growing nanoparticles.<sup>27</sup> It was found that homogeneous mixing of all metals in the final high entropy alloy nanoparticle products could be achieved by choosing reaction times and temperatures that accounted for differences in reduction potentials and rates of reduction. When the 3d transition metal Ni was replaced with Sn, a representative p-block element, the same synthetic protocol used to make NiPdPtRhIr produced SnPdPtRhIr, but through a different mechanism.<sup>27</sup> Here, time-dependent studies showed evidence of simultaneous reduction and incorporation of all elements rather than initial formation of a metal-rich seed. The synthesis of NiSnPdPtIr, which contains both Ni and Sn and therefore introduces a potential competition between the two pathways, adopted a pathway that combined aspects of both. PdSn-rich NiSnPdPtIr nanoparticles were observed early in the reaction, suggesting that Sn may have inhibited the Pd-rich PdNi seed pathway and instead triggered the simultaneous reduction of all the other metal reagents.<sup>27</sup>

The studies highlighted above point to the “heterogeneous” reaction pathways that ultimately (ideally) lead to homogeneously alloyed products. The nominally one-pot reactions that might be assumed to proceed by simultaneously coreducing and combining all elements into the growing nanoparticle can instead proceed in stages. In these pathways, seeds that are rich in one or two metals form first and incorporate other metals in different ways and at different times, eventually producing the targeted alloy nanoparticle, although often with some heterogeneity that is likely to be a relic of how they are synthesized. Validating this approach, the one-pot slow-injection synthesis of high entropy intermetallic (Pd, Rh, Ir, Pt)Sn nanoparticles proceeds through a conceptually similar stepwise process. However, a 1:4 ratio

of each metal to tin was critical to access the intermetallic phase, while a 1:1 ratio of each metal to tin favors the corresponding alloy phase. Pd-rich Pd–Sn cube-shaped seeds form first, and then the other metals deposit onto the corners and grow outward, ultimately forming flowerlike morphologies.<sup>29</sup> Throughout this process, tin continues to incorporate and diffuse throughout the growing particles, homogenizing the composition distribution as the reaction progresses.<sup>29</sup>

Other examples of colloidal high entropy alloy nanoparticle formation that have been reported also point to complex reaction chemistry and/or multistep pathways. For example, it was found that the spatial composition distribution and morphology of high entropy alloys could be predicted based on knowledge of the relative rates of reduction of the metal salts used to synthesize them.<sup>52</sup> These insights allowed tuning of the morphology as well as the formation of core–shell nanoparticles such as Pd@PdPtRhIrRu when a Pd core formed first due to its faster reduction kinetics,<sup>52</sup> which is consistent with the behavior identified in previous mechanistic studies.<sup>27,29,43</sup> During the synthesis of PtFeNiCuMoRu high entropy alloy nanoparticles, only a small amount (~1%) of Ru was present, but its presence was crucial for controlling the shapes of the nanoparticles.<sup>53</sup> Likewise, addition of the p-block metals Bi and Sn can lead to the formation of core–shell high entropy alloy nanoparticles of platinum group metals, as demonstrated for the synthesis of PdPtAgBiSn having a Pd-rich core and a Pt-rich shell.<sup>54</sup> Time-dependent studies revealed that the reaction started with coreduction of all metals, although Pd and Ag were the dominant species due to their high reduction potentials and fast reduction kinetics; the other metals were reduced more slowly and incorporated over time, with spatial distributions and phase segregation depending on the rates of deposition and growth.<sup>54</sup>

Mo(CO)<sub>6</sub> was found to be an important reagent in forming high entropy alloy nanoparticles such as PdFeCoNiCu,<sup>55</sup> PtFeCoNiCu,<sup>44</sup> and RuFeCoNiCu.<sup>56</sup> While Mo(CO)<sub>6</sub> was used as a reducing agent, the fate of the Mo is unknown, as is its potential role in the reaction mechanism. While Mo was not incorporated into the high entropy alloy nanoparticles in these examples, it was incorporated when Mo(CO)<sub>6</sub> was used to synthesize PdMoGaInNi,<sup>57</sup> PtFeNiCuMoRu,<sup>53</sup> PtRuNiCoFeMo,<sup>58</sup> and PtRhIrRuCoFeNiMnCrMo.<sup>59</sup> Studies have pointed to the role of Mo(CO)<sub>6</sub> in directing nanoparticle shape and in reducing certain elements, such as Cr and Ru,<sup>59</sup> although other reports indicate incorporation of Cr<sup>60</sup> and Ru<sup>26</sup> without the need for Mo(CO)<sub>6</sub>. Interestingly, it was found that the reaction also proceeded through the formation of an initial Pt core nanowire onto which the other elements were reduced and alloyed.<sup>59</sup> This observation merges key aspects of the previously discussed pathways, which involve initial rapid formation of a noble metal core followed by autocatalytic deposition and incorporation of other metals, with those involving small amounts of reactive metals, such as Mo(CO)<sub>6</sub>. The take-away message is that Mo(CO)<sub>6</sub> clearly plays a role in the synthesis of several types of high entropy alloy nanoparticles depending on the constituent elements and other components of the reaction, yet its specific role is clearly complex and not fully understood. All of these examples—with and without Mo(CO)<sub>6</sub>—highlight the complex reaction chemistry that is involved in forming colloidal high entropy alloy nanoparticles and the need to identify and understand mechanistic insights so that composition, homogeneity, and morphology can be controlled and tuned.

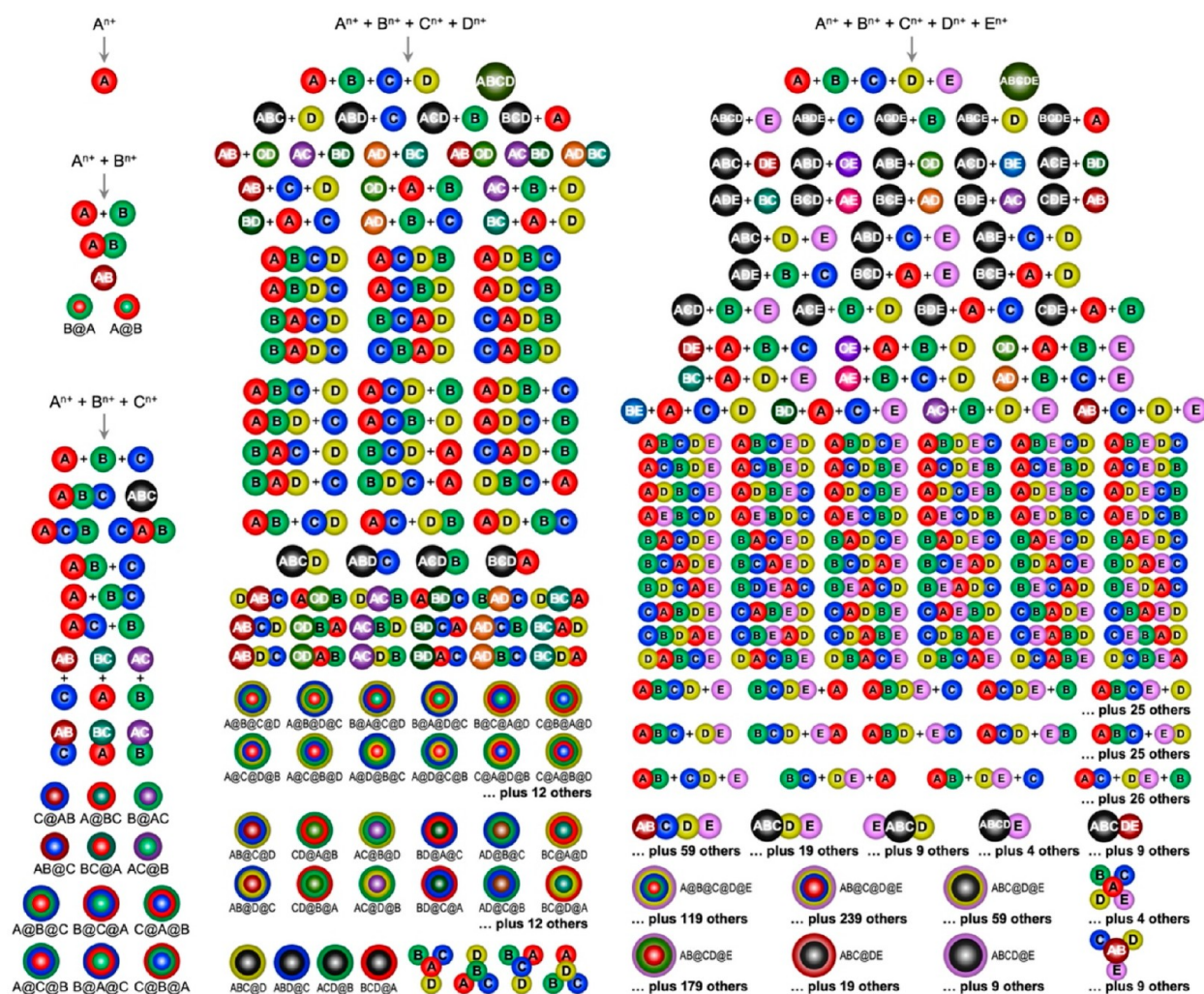


**Figure 3.** Overview of all possible reaction outcomes for unary, binary, ternary, quaternary, and quinary combinations of metals that can lead to the formation of individual discrete single-metal and alloy nanoparticles, various interconnected multicomponent heterostructures, and core–shell particles. Other combinations are possible; these variants emphasize the most likely products based on current knowledge of colloidal nanoparticle chemistry. For the quinary system, accessing the high entropy alloy product requires finding a reaction pathway that selects for it exclusively, relative to the hundreds of other possible products.

Given the chemical challenges associated with the concurrent reduction and mixing of different elements with different reduction potentials and different reduction kinetics, an alternative strategy is to purposely begin with nanoparticle seeds of one or more metals and then deposit other metals in a controlled manner on them, followed by annealing to induce diffusion and alloying. Rather than relying on five or more elements reacting to form a single product in a single-pot reaction, phase-segregated products can be readily synthesized and used as precursors that transform into single-phase high entropy alloys. The initial demonstration of this seed-mediated coreduction approach involved the colloidal synthesis of intermetallic PdCu nanoparticles, which were used as seeds to galvanically deposit a PtNiCo alloy shell to form PtNiCo@PdCu. When annealed after anchoring the particles on a refractory support, the core–shell particles were transformed to PdCuPtNiCo high entropy alloy nanoparticles.<sup>44,45</sup> This approach has been expanded to compositionally more complex alloys, including PdCuPtNiCoRh and PdCuPtNiCoRhIr.<sup>45,46</sup> A related galvanic deposition approach used a Ag nanowire template to trigger galvanic exchange with other more noble metals, followed by a dealloying step that mixed all of the

metals. The products included PtPdIrRuAuAg, PtPdIrRuAuRhAg, and PtPdIrRuAuRhOsAg high entropy alloy nanowires.<sup>61</sup>

### ■ HOW DO WE NAVIGATE COMPLEX REACTION PATHWAYS AND COMPETING CHEMICAL REACTIVITIES?

As is clear from the brief survey of the literature on synthesizing colloidal high entropy alloy nanoparticles that was provided in the preceding section, chemical reactivity plays a central role in the success or failure of a reaction. The key to being able to synthesize colloidal nanoparticles of high entropy materials without requiring a high-temperature annealing step that pyrolyzes ligands and compromises their colloidal stability is to adequately deal with the complex and competing chemical reactivities associated with the large number of reagents and possible products (Figure 3). Consider the solution-phase synthesis of colloidal noble metal nanoparticles. We now know that every aspect of a synthetic protocol matters in achieving a desired outcome: the metal reagents (including their oxidation states, counterions, and/or ligands), reducing agents, solvents, additives (ligands, polymers, and/or salts), how the reagents

are added (one pot from the beginning, slowly injected, rapidly injected, sequentially), reaction temperatures, reaction times, heating rates, cooling rates, and/or other variables.<sup>62,63</sup> These considerations are for one metal. These same variables matter for a successful synthesis of bimetallic alloy nanoparticles as well, although additional considerations are necessary to ensure that the metals mix homogeneously rather than nucleate and grow independently as separate nonalloyed metal nanoparticles. The key here is to balance reactivities and the rates of the various processes through judicious choice of reagents and reaction variables. It is also important to avoid competing pathways such as galvanic exchange, which can occur for two metals that have significantly different reduction potentials, or the formation of core–shell particles, if one metal is reduced significantly faster than the other.

For high entropy materials, which have many more metals present at the same time, the cross-reactivities and alternate reaction outcomes can become immensely more complicated. Building from the single-metal and bimetallic cases described above, let us now consider an alloy nanoparticle containing five metals, as is the typical case for a so-called high entropy alloy nanoparticle. Each step of a mechanism will have a rate constant associated with it. Additionally, for each metal reagent, the rate will depend on the type of reaction needed for it to form a reactive metal species in solution, such as decomposition, ligand dissociation, and/or reduction from a cationic metal species, which will have different reduction potentials depending on the ligands and coordination geometry in solution. These reactivity considerations make it challenging to balance reactivities such that all five metal reagents react and combine simultaneously in the nucleating and growing nanoparticle, which disfavors a pathway involving simultaneous incorporation of five or more metals during nanoparticle growth. At the same time, if one or more metals that incorporate into the growing nanoparticle are less noble than one or more metals remaining in solution, a galvanic replacement pathway could be triggered. In such a case, the more noble metals would be reduced onto the surface of the growing nanoparticle as the less noble metals already incorporated into the nanoparticle would oxidize and subsequently solubilize, leaving the nanoparticle. If the reaction environment is sufficiently reducing, a pathway where reductive deposition occurs could compete with, or complement, a galvanic process. It is also possible to envision a seeded growth pathway if one or more metals is reduced first to form primary nanoparticles (seeds) that then catalyze the deposition of the other metals as a shell, perhaps through an underpotential deposition process. This approach can lead to core–shell particles, which could also diffuse into a homogeneous alloy depending on the reaction temperature.

All of the hypothetical cases mentioned above, which are only a few of many possibilities one can envision in a five-metal system, have been observed and/or postulated, and all are reasonable. In many cases, there is evidence for multiple pathways occurring at different stages of the reaction, which is not unexpected given the evolution of nanoparticles discussed above as well as how the relative reactivities among the nanoparticles and the solubilized reagents can change as the reaction progresses. In many cases, reaction pathways remain unknown, as it can be challenging and laborious to identify diagnostic characteristics. The point is that there is inherent complexity in the solution-phase reactions that lead to the formation of colloidal high entropy nanoparticles, as is

expected given the number of variables and reagents, some of which are independent and many of which are correlated in unknown ways. It is therefore important to acknowledge this complexity in reactions and reactivity, especially the reality of multiple and competing reactions and reaction pathways that can change as the reaction progresses. Because of this complexity, synthetic development is well-suited for Bayesian optimization, Design of Experiments, machine learning, and other automated strategies capable of handling multiple variables, as these methods can help to accelerate the identification of reaction parameters that lead to products with targeted features having the highest possible yields and purities.<sup>63,64</sup>

### ■ IS THE FORMATION OF COLLOIDAL HIGH ENTROPY NANOPARTICLES REALLY DUE TO ENTROPY?

The classical definition of high entropy stabilization is driven by the configurational entropy of mixing ( $\Delta S_{\text{mix}}$ ), which is defined according to eq 1:

$$\Delta S_{\text{mix}} = -R \sum_i x_i \ln x_i \quad (1)$$

where  $R$  is the ideal gas constant and  $x_i$  is the mole fraction of the  $i$ th component in the system. Equal contributions to the mole fraction from all the components would maximize  $\Delta S_{\text{mix}}$ . For a five-component system, the configurational entropy of mixing is 1.6 $R$ , which is greater than the conventionally agreed upon minimum threshold of 1.5 $R$  required for entropy stabilization, which was defined based on observation. However, at low temperatures, which we consider to be <350 °C due to the typical range of solvent-accessible temperatures during colloidal synthesis,  $\Delta S_{\text{mix}}$  cannot provide enough stabilization on its own, but combined with high temperatures it can overcome the enthalpic penalties associated with mixing. Colloquially, the working definition of “high entropy” is often simplified to alloys having five or more elements, each comprising atomic percentages between 5 and 35% randomly distributed throughout a crystal lattice, as such systems generally satisfy the 1.6 $R$  criterion.<sup>1</sup> However, not all alloys containing five or more randomly distributed metals form, or are stabilized, due to entropic effects. Such systems can therefore more accurately be described by terms such as multiprincipal element alloys or complex solid solutions, as has been discussed in the literature. However, guidelines continue to evolve,<sup>3</sup> and the broader community often uses expanded definitions. Therefore, in most cases, crystalline alloys that incorporate five or more elements, each having atomic percentages of 5–35%, are generally referred to as high entropy alloys.

Here we turn to the idea of entropy stabilization, which is sometimes assumed to be the driving force by which high entropy nanoparticles form based on the colloquial definition, whether correct or incorrect. Interestingly, the concept of entropy stabilization is largely incompatible with the reality of the solution routes that are used to synthesize colloidal high entropy nanoparticles. Put another way, for the  $\Delta S$  term to be non-negligible relative to  $\Delta H$ , even if there is a high configurational entropy due to randomization of five or more elements on a crystalline lattice site, the temperature must be high because of  $\Delta G = \Delta H - T\Delta S$ . Colloidal nanoparticle synthesis methods occur at temperatures less than or equal to



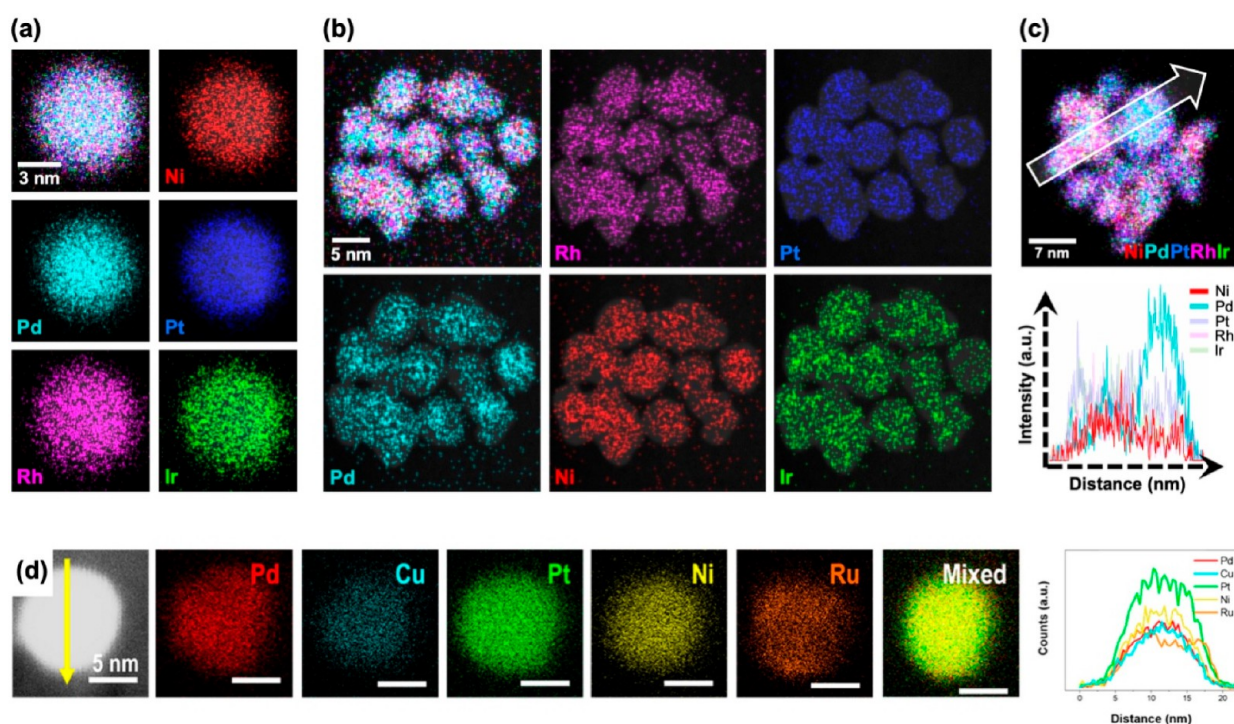


**Figure 4.** Microscopy data highlighting heterogeneities in high entropy alloy nanoparticles. Panels (a) and (b) show STEM-EDS maps for a single particle and a collection of particles with the composition  $\text{Ni}_{0.19}\text{Pd}_{0.21}\text{Pt}_{0.22}\text{Rh}_{0.20}\text{Ir}_{0.18}$ . The data in (a) suggest a homogeneous distribution of all five elements throughout the particle. The data in (b), however, reveal some compositional inhomogeneity throughout the particles. In (c), inter- and intraparticle heterogeneity is clearly observed in a minor subpopulation of the same sample shown in (a) and (b). (d) STEM-EDS maps for a single PdCuPtNiRu nanoparticle. Intraparticle heterogeneity can be observed in the center of the nanoparticle, where the relative amount of Ru is lower compared to the edges, as verified by the line scan. Panels (a–c) are adapted from ref 27. Copyright 2023 American Chemical Society. Panel (d) is adapted from ref 46. Copyright 2022 American Chemical Society.

the reflux temperatures of high-boiling-point solvents, which are generally  $\leq 350$  °C, as mentioned above. In contrast, most bulk high entropy materials are synthesized at much higher temperatures. This comparison implies that colloidal synthesized nanoparticles may not form due to entropy considerations, as the temperature is insufficiently high for the  $T\Delta S$  term to overcome the enthalpic penalty. If a sample of high entropy nanoparticles is heated to a high temperature and then phase-segregated upon slow cooling but not upon rapid quenching, then it is likely to be entropy-stabilized.<sup>6</sup> In the end, though, it is important to recognize the distinction between “high entropy” as a broad definition relating to compositional complexity and “entropy stabilization”, which implies a thermodynamic driver.

Despite the discussions in the previous paragraphs, there still is much that we do not yet know about colloidal high entropy nanoparticle systems, so it is premature to draw conclusions and inferences simply based on comparisons with traditional bulk compounds and synthetic methods. For example, surface energy, which is negligible in bulk crystals, contributes significantly to the overall energy of a nanoparticle. The solution-phase colloidal synthesis platform also introduces enthalpic and entropic contributions that are not present in bulk-scale reactions that occur fully in the solid state, including solvation, precipitation, and ligand dissociation from metal complexes, which involves breaking bonds and releasing into solution ligands that were previously confined around a metal center. Additionally, different reaction pathways can have different combinations of enthalpic and entropic factors. As an example, in the synthesis of (Zn, Co, Cu, In, Ga)S using cation

exchange,<sup>32</sup> crystalline  $\text{Cu}_{1.8}\text{S}$  nanoparticles are synthesized first. Then, in a subsequent step, after the crystalline lattice is already defined, the  $\text{Cu}^+$  cations are released from the crystal into solution while other cations from solution are desolvated and enter the crystal. The solvation and desolvation processes lend significant enthalpic contributions, which are major driving forces for cation exchange. At the same time, for the divalent and trivalent cations that exchange for  $\text{Cu}^+$ , two or three  $\text{Cu}^+$  cations are solvated for every  $\text{M}^{2+}$  or  $\text{M}^{3+}$  cation that is desolvated, which together constitutes a large entropic contribution.<sup>32</sup> Because of the considerations discussed above, we are not yet in a place to say definitively whether colloidal high entropy nanoparticles form or are stabilized due to entropy or specify the relative contributions of enthalpy versus entropy. This question remains open and will require more in-depth mechanistic studies as well as advances in computational capabilities that can handle the large number of independent and correlated variables, both in the materials and in the pathways by which they are synthesized, as well as the compositional and structural complexity of the high entropy materials.

#### ■ HOW DO WE DESCRIBE THE MIXING OF ELEMENTS IN COLLOIDAL HIGH ENTROPY NANOPARTICLES?

The idealized model of a high entropy alloy has all metals perfectly randomized among the available lattice sites of a crystalline compound. However, much remains unknown about how the elements really mix, both within the nanoparticles and on their surfaces. Evidence is mounting

that heterogeneities are potentially quite common, with some amount of segregation coexisting with randomized regions within nanoparticles (Figure 4).<sup>27,45</sup> Some of these heterogeneities could come from inherent mixing limitations or possibly point to formation and stabilization that are not due to entropy effects. Some of these heterogeneities could arise from trapping an intermediate state that is neither fully segregated nor fully mixed. Some of these heterogeneities could also result from the pathways in which colloidal nanoparticles of high entropy materials are formed, especially if one or more elements nucleates and begins to grow first, serving as a seed onto which the other metals subsequently deposit.<sup>27</sup> Similarly, we know almost nothing about the surface composition of colloidal high entropy alloy nanoparticles. Conventional alloy nanoparticles often exhibit some degree of surface segregation of reactivity. For example, in some alloy nanoparticles, the more noble metal segregates to the surface,<sup>65</sup> while in others, the more oxophilic metal oxidizes and forms an oxide shell.<sup>66</sup> In other cases, surface segregation can be impacted by the stabilizing ligands and change dynamically depending on the reactivity (i.e., oxidizing or reducing) of the environment.<sup>67</sup>

### ■ WHAT CHARACTERIZATION CHALLENGES EMERGE WITH HIGH ENTROPY NANOPARTICLES?

Given their compositional complexity, the complex and competing chemical reactivities that are an inherent part of their synthesis, and their small sizes, colloidal nanoparticles of high entropy materials can be challenging to characterize. Additionally, unique aspects of high entropy nanoparticles complicate the analysis and interpretation of mainstream materials characterization techniques that are routinely used for nanoparticles. At a minimum, given the instrumentation that is most commonly available to nanoparticle researchers and that is most often used by this community, it is important to adequately characterize composition and spatial distributions, including a statistically significant number of individual particles and a sufficiently large ensemble of particles to mimic the bulk sample, if not the bulk sample itself. Additionally, it is also important to characterize crystal structure and to compare lattice constants to those expected based on the composition. Finally, it is important to characterize phase purity versus segregation.

Below, we highlight some of the unique aspects that must be considered for colloidal nanoparticles of high entropy materials when characterizing them using electron microscopy and X-ray diffraction (XRD), which are among the most commonly available and utilized techniques for nanoparticles. First and foremost, it is important to have foundational knowledge about these techniques and how they work as well as the data that they generate and how the data are analyzed—both automatically by the instrument's software and manually by the user. Many examples exist in the rapidly growing literature on nanoparticles of high entropy materials where inaccurate conclusions are drawn based on improper or inadequate data analysis.

#### Electron Microscopy

Conventional transmission electron microscopy (TEM) imaging provides information about particle shape, size, and uniformity, and coupling it with energy-dispersive X-ray spectroscopy (EDS) provides information about the composition of the ensemble of particles imaged. High-angle annular

dark-field scanning TEM (HAADF-STEM) coupled with EDS mapping (STEM-EDS) can provide high-resolution images of individual particles with overlaid element maps showing detailed information about how the elements are distributed through a two-dimensional projection of a particle. Here we focus on issues associated with characterization of the composition and composition distribution, as these are where challenges emerge due to the unique aspects of high entropy materials. First, STEM-EDS can be used to determine the compositions of individual particles imaged at high magnification and resolution as well as how the various elements are distributed throughout individual particles. Such analyses will confirm colocalization of all elements at the single-particle level as well as indicate whether they are homogeneously or heterogeneously mixed. STEM-EDS element maps provide two-dimensional visual depictions of how the various elements are distributed, while line scans allow for a more detailed comparative analysis as well as eliminating bias due to perceived intensity differences due to color choice rather than signal.

Ensemble EDS is useful for confirming that the compositions observed for single particles match a larger subpopulation of the sample or to identify heterogeneities among particles (Figure 5a). Complementary bulk analysis, such as inductively coupled plasma with mass spectrometry (ICP-MS), can further confirm that the composition observed microscopically matches the compositions of individual particles and ensembles, with the caveat that bulk elemental analysis alone cannot distinguish between physical mixtures of phase-segregated nanoparticles versus nanoparticles of homogeneously mixed elements (Figure 5b). X-ray photoelectron spectroscopy (XPS) can help to further confirm composition, with the caveats that it focuses on the surface, which may have a different composition, and that it also evaluates a large swath of the sample rather than individual particles. Scanning electron microscopy (SEM) with EDS can be useful for intermediate-scale composition analysis, but it is important to recognize that it is neither a bulk technique, as it still analyzes only a microscopic portion of the sample, nor capable of particle-by-particle analysis and therefore cannot provide information about composition distributions and homogeneity versus heterogeneity within single particles or ensembles of them.

STEM combined with electron energy loss spectroscopy can provide additional information that is complementary to STEM-EDS about how the elements mix at the atomic level as well as information about their coordination environment, bonding, and oxidation states.<sup>68</sup> Another complementary element-specific bulk technique that provides insights into composition and electronic structure is X-ray absorption spectroscopy (XAS). X-ray absorption near edge structure (XANES) can be used to elucidate the electronic structure and interactions of an element with neighboring atoms, along with their oxidation states.<sup>69,70</sup> Extended X-ray absorption fine structure (EXAFS), on the other hand, provides information about the local coordination environment and interatomic distances.<sup>70</sup> These techniques, while powerful, require synchrotron facilities and therefore are less widely utilized than the microscopy, diffraction, and surface spectroscopy techniques mentioned above. Overall, bulk, multiparticle, and single-particle analyses are complementary and useful in combination. It is important to remember that bulk composition analysis without composition analysis of single

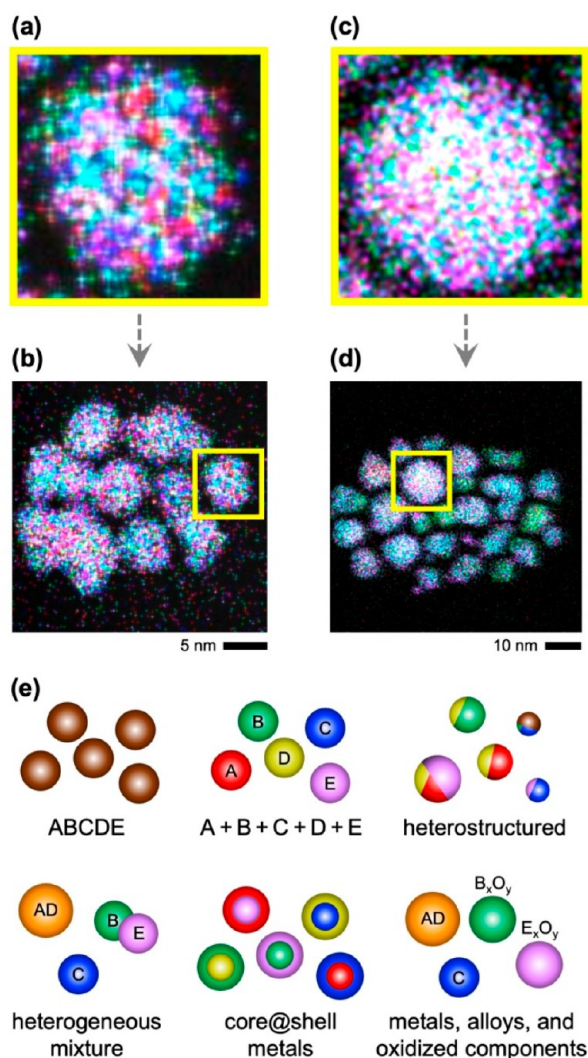


**Figure 5.** (a) Overlaid STEM-EDS element map of a single  $\text{Ni}_{0.19}\text{Pd}_{0.21}\text{Pt}_{0.22}\text{Rh}_{0.20}\text{Ir}_{0.18}$  nanoparticle, highlighting the homogeneous distribution of all elements. (b) STEM-EDS element map for the larger collection of nanoparticles from which the single-particle image in (a) was cropped, as indicated with the yellow box. This image indicates that the homogeneous distribution of elements observed in the single particle is also present across multiple particles. (c) Overlaid STEM-EDS element map for another single  $\text{Ni}_{0.25}\text{Pd}_{0.18}\text{Pt}_{0.21}\text{Rh}_{0.19}\text{Ir}_{0.17}$  nanoparticle, synthesized under different conditions than the sample shown in (b), taken from the image in (d), as indicated with the yellow box. Here, the larger collection of nanoparticles has significant particle-to-particle heterogeneity, making the cropped particle in (c) nonrepresentative of the data in (d). (e) Cartoon depiction of several distinct combinations of five metals (A, B, C, D, E) that can arise during the synthesis of high entropy alloys. All six types of samples in (e) could have identical compositions using bulk techniques, such as ICP-MS, which average across the entire sample and do not account for how the elements are distributed within nanoparticles. Panels (a) and (b) are adapted from ref 27. Copyright 2023 American Chemical Society.

particles and particle ensembles does not provide the full picture, nor does particle-level composition analysis without complementary bulk analysis.

When using EDS analysis and STEM-EDS element mapping, three considerations are important, but sometimes overlooked, for high entropy nanoparticles. First, the STEM-EDS element maps are most frequently presented as a

composite image that overlays all of the individual element maps. This approach quickly conveys the extent of colocalization of the elements through simple visual observation. However, in these maps, each element is assigned a color, and the different colors can appear lighter or darker or have higher or lower contrast relative to one another simply based on their hue, value, and saturation—key aspects of color that are unrelated to any aspect of quantification of element ratios (Figure 6a). However, the human eye often wants to interpret color-coded data as being relevant to quantities that it may represent. Following this logic for overlaid STEM-EDS element maps for high entropy nanoparticles, elements represented by brighter colors with higher contrast would be thought to have higher atomic ratios while elements represented by darker colors with lower contrast would be thought to have lower atomic ratios. Additionally, software can sometimes normalize (intentionally or unintentionally) the intensities of the colors, which results in highly qualitative maps that further distort any intended visual perception of relative atomic ratios. As a result of these considerations, a purely visual analysis of STEM-EDS maps is flawed from the perspective of quantifying the relative ratios of the elements, despite its utility in visualizing spatial colocalization. This issue makes it important to look at line scans or other data presentation methods that convey the spatial distribution of atomic percentages in an unbiased way. However, one needs to be mindful of how the line scans are acquired and presented. For example, if the width of the line that is scanned spans the entire nanoparticle, the resulting data will be more equivalent to ensemble data for the particle that will not capture nanoscale heterogeneities or clustering. In contrast, a line scan with a narrower width that samples slices of the nanoparticle will have lower signal than a thicker line scan but may allow better visualization of any potential heterogeneity or clustering in certain regions. Presenting the non-overlaid individual STEM-EDS maps for each element is also useful to show the spatial distributions for each element, to look for clustering of two or more elements, and to allow those who experience color blindness to see the data for each element without requiring color.

A second challenge is with low signals, which can appear spread throughout a STEM-EDS element map and can often be even more pronounced in the region where a particle is located (Figure 6b). It is therefore important to verify, through comparison with ensemble spectra, that the element is indeed present at above-baseline levels that are appropriate for designation as a high entropy material. Some software packages for STEM-EDS mapping can falsely map the presence of certain elements if their lines overlap with an actual element present in the sample, as is the case for Rh  $L\beta$  and Pd  $L\alpha$ , which overlap (Figure 6b). Even in the absence of overlapping lines, signal above the “corrected” background can sometimes be construed as real data, which can lead to erroneous maps. However, other software packages can better deconvolute overlapping lines and background signal, thereby minimizing such discrepancies. For these reasons, it is important to know how the mapping software functions to ensure accurate data presentation and interpretation. As an additional consideration, the use of unusually large pixels in maps that show the spatial distribution of elements can mask their true distribution and not allow heterogeneities or clustering to be visualized.

A third important consideration for STEM-EDS composition analysis and/or element mapping of high entropy

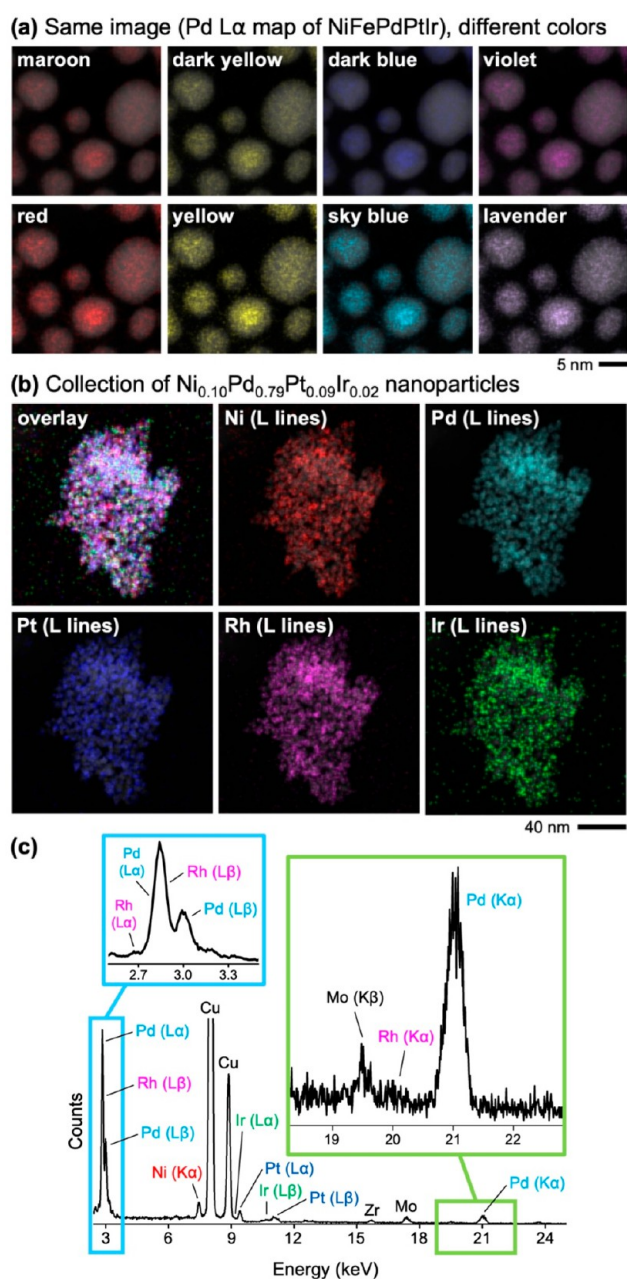


**Figure 6.** (a) HAADF-STEM image with overlaid Pd  $L\alpha$  STEM-EDS map for a small collection of high entropy alloy nanoparticles having an average composition of  $\text{Ni}_{0.19}\text{Pd}_{0.21}\text{Pt}_{0.22}\text{Rh}_{0.20}\text{Ir}_{0.18}$ . The images in different panels are identical, but the colors of the STEM-EDS map vary, which can lead to erroneous predictions of the composition based only on visual inspection. (b) HAADF-STEM image with overlaid STEM-EDS maps of Ni, Pd, Pt, Rh, and Ir for nanoparticles having an average composition of  $\text{Ni}_{0.10}\text{Pd}_{0.79}\text{Pt}_{0.09}\text{Ir}_{0.02}$ . The Rh  $L\beta$  and Pd  $L\alpha$  lines overlap, leading to the erroneous visual appearance of Rh in a sample that is composed only of Ni, Pd, Pt, and Ir. Additionally, the relative brightness and contrast of the STEM-EDS maps do not correlate with the amount of each element present, which requires analysis of the corresponding EDS spectrum to adequately evaluate. (c) EDS spectrum for the sample in (b) with each peak labeled to show which elements are and are not present as well as those that overlap. Enlarged regions near energies of 3 and 21 keV are outlined in blue and green, respectively. Cu is from the TEM grid, Mo is from the TEM clips, and Zr is adventitious. The panels in (a) are adapted from ref 27. Copyright 2023 American Chemical Society.

nanoparticles is careful attention to which EDS lines are used (Figure 7). For some elements, the X-ray lines most commonly used in EDS analysis can overlap, as mentioned above, which complicates analysis. This overlap is particularly problematic for high entropy nanoparticles, if analyzed improperly, because false positives can emerge. That is, the presence of overlapping X-ray lines can lead to the erroneous conclusion that two elements are present when only one is, resulting in incorrect compositions. Figure 7 highlights this issue when analyzing a nanoparticle of  $\text{Zn}_{0.25}\text{Co}_{0.22}\text{Cu}_{0.28}\text{In}_{0.16}\text{Ga}_{0.11}\text{S}$ , where false signals attributed to Ag, Cd, Ir, Os, Pt, Sn, and W are mapped in addition to true signals from the real elements, which are Zn, Co, In, Ga, and Cu. In this case, overlapping X-ray lines and/or incorrect background correction by the software leads to false signal that is concentrated on the particle. While the newest software offers powerful deconvolution features, it is important to not assume that such automated analysis carries out deconvolution sufficiently well to provide adequate elemental ratios; it is up to the user to verify. It is also imperative to disclose which EDS lines were mapped and/or used for quantification and how they were analyzed so that this issue is acknowledged and mitigated.

### X-ray Diffraction

XRD provides useful information about the crystalline phases that are present in a sample as well as the possible presence of significant amounts of amorphous material. XRD can also provide information about grain sizes and features such as crystallinity, strain, and morphology.<sup>71</sup> For nanoparticles of high entropy materials, XRD is most commonly used to evaluate phase purity. The majority of colloidal nanoparticles of high entropy materials that have been synthesized to date adopt somewhat simple crystal structures, such as hcp and fcc alloys, rocksalt and spinel oxides, and NiAs and related binary intermetallics. XRD patterns of nanoparticles have peaks that are broadened due to the smaller crystalline grain sizes. Crystalline impurities that differ in structure from those of the high entropy phase are therefore reasonably straightforward to detect by XRD in most cases, provided that the signal-to-noise ratio of the XRD pattern is sufficiently high. Significant amounts of amorphous impurities may also be observed through broad above-background features and should be verified using SEM or other techniques. The most common use of XRD for solution-synthesized nanoparticles of high entropy materials is to confirm that the bulk sample consists primarily of a single crystalline phase.

The literature is replete with examples of XRD patterns for colloidal synthesized high entropy nanoparticles that show evidence of phase segregation, despite claims to the contrary. In many cases, such interpretations arise because the XRD patterns have an unacceptably low signal-to-noise ratio such that peaks, including impurity peaks, cannot be adequately resolved. In other cases, atypical peak shapes that are characteristic of multiphase samples are idealized and interpreted as a single peak when they actually correspond to a superposition of multiple peaks. Common XRD characteristics that inform about phase identification, phase purity, composition, and nanoparticle size include peak symmetry, peak broadening, and the ability to account for all of the peaks that are present in an XRD pattern.<sup>71</sup>

Phase-pure nanoparticle samples of high entropy materials will have largely symmetric peaks. Additionally, peak widths will be consistent with those expected from the Scherrer

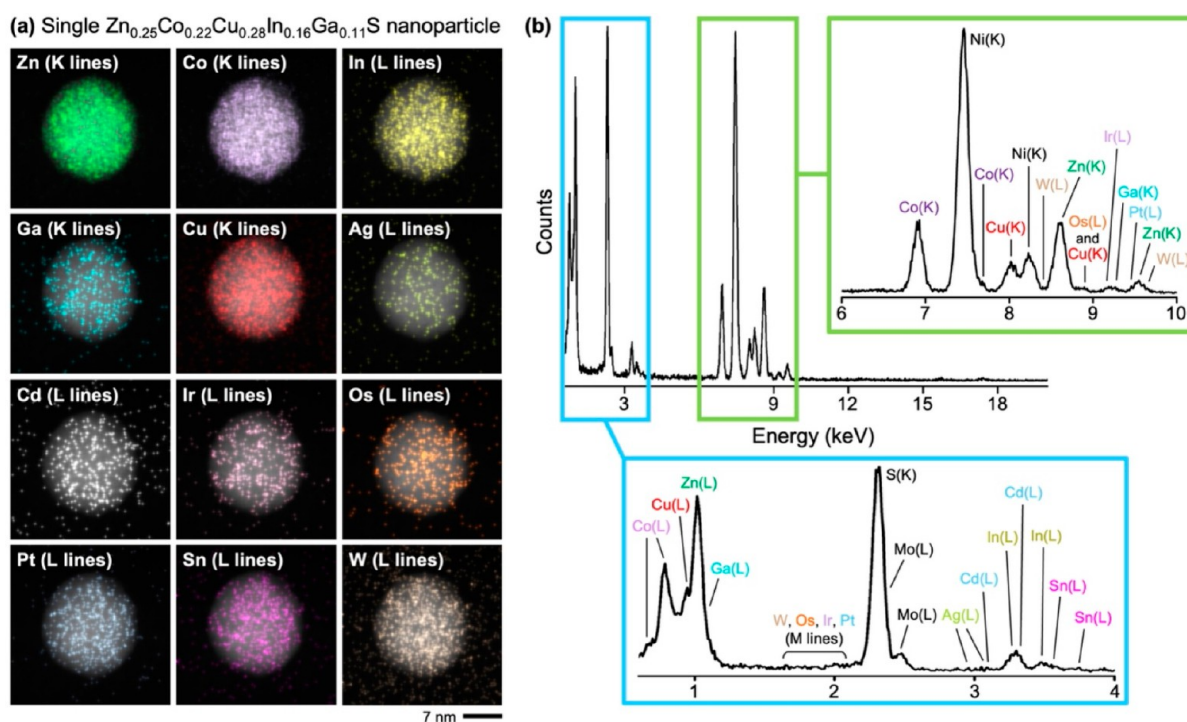


**Figure 7.** (a) STEM-EDS element maps overlaid on a HAADF-STEM image for a single  $(\text{Zn}, \text{Co}, \text{In}, \text{Ga}, \text{Cu})\text{S}$  high entropy metal sulfide nanoparticle. The signals from Zn, Co, In, Ga, and Cu are real, whereas those from Ag, Cd, Ir, Os, Pt, Sn, and W are erroneous due to the presence of overlapping energy lines in the EDS spectrum and/or the interpretation of background signal as real. (b) The corresponding EDS spectrum, highlighting all lines for the elements displayed in the maps in (a). Enlarged regions below 4 keV and between 6 and 10 keV are outlined in blue and green, respectively. Ni is from the TEM grid, and Mo is from the TEM clips. This figure is adapted from ref 32. Copyright 2021 American Chemical Society.

equation based on the average particle size observed by TEM, as long as HRTEM confirms that the nanoparticles consist of single-crystalline domains. The XRD pattern is often used as a fingerprint to confirm that it matches a reference. However, most high entropy materials do not yet have available references, so it is difficult to precisely benchmark based on available databases of powder XRD patterns. Simulated powder XRD patterns can be constructed using the observed crystal structure, i.e., fcc if the pattern qualitatively matches that of a constituent fcc metal, with lattice parameters estimated using Vegard's law based on the experimentally determined composition of the high entropy material. Vegard's law corresponds to a weighted average of the end members and therefore provides an estimate of the lattice parameters that should be observed by XRD, given the composition observed by EDS or other technique, assuming that the microscopic and macroscopic analyses are self-consistent. For end members that may not exist by themselves in the crystal structure adopted by the high entropy material, a source like Materials Project<sup>72</sup> may provide a reasonable computed alternative to experimental data that can be used in such cases. Ultimately, the experimental lattice parameters may still be slightly different from those that are estimated due to strain and other effects, but this approach provides a reasonable starting point and helps to add semiquantitative correlation among techniques. Selected-area electron diffraction can further close the loop by confirming that the nanoparticles analyzed microscopically are crystalline, have the same crystal structure, and are single-phase, with lattice constants that match those observed by XRD.

Figure 8 shows three simulated XRD patterns of “high entropy alloy” samples based on an fcc crystal structure, which highlights some of the intricacies involved in analyzing an XRD pattern of high entropy alloy nanoparticles. For crystal structures having lower symmetries and/or larger unit cells, including most of those shown in Figure 1, these issues encountered during analysis of the XRD patterns will be exacerbated because of the presence of a larger number of peaks, some of which will be close together.<sup>71</sup> In Figure 8, the black-colored diffraction pattern at the bottom corresponds to a single-phase fcc high entropy alloy having a composition of NiPdPtRhIr and a grain size of 5 nm.<sup>27</sup> All peaks expected for an fcc crystal structure are present in the correct relative ratios. Further, the peaks are symmetric but broadened due to the small crystallite size.<sup>71</sup> The red-colored pattern in the middle corresponds to a quaternary alloy having a composition of NiPtRhIr, along with 20% Pd present as a separate phase; both NiPtRhIr and Pd are modeled as fcc phases with 5 nm grain sizes. This simulated XRD pattern represents a phase-segregated sample where one of the metals does not mix with the others. Asymmetry in the (111) and (200) peaks is evident, which is consistent with the presence of two fcc phases having similar (but distinct) lattice constants. Phase segregation is especially obvious at higher  $2\theta$  values, as the distinct shoulders due to the second phase (Pd) are evident. If only a very small amount of Pd is phase-segregated, the asymmetry and appearance of a shoulder are less obvious, especially in a real XRD pattern due to background noise. This situation is especially complicated when there is intraparticle heterogeneity, which may lead to very broad peaks of the minor segregated phase that can be difficult to observe due to

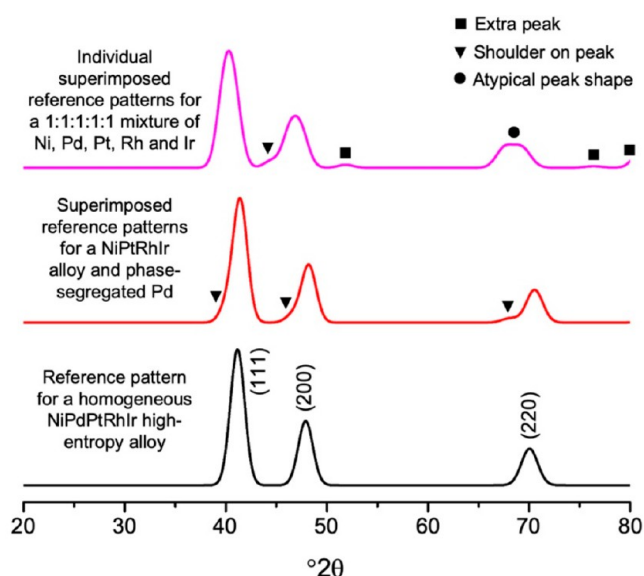


**Figure 8.** Simulated XRD patterns for various samples related to nanoparticles of a NiPdPtRhIr high entropy alloy. The bottom, black-colored pattern corresponds to a single-phase fcc NiPdPtRhIr equiatomic high entropy alloy with a grain size of 5 nm. The middle, red-colored pattern corresponds to a 5 nm quaternary NiPdPtRhIr alloy with a 20% impurity of 5 nm Pd, representing phase segregation of the elements in an attempted high entropy nanoparticle synthesis. The top, magenta-colored pattern corresponds to an equiatomic mixture of 5 nm Ni, Pd, Pt, Rh, and Ir, representing complete phase segregation of all five constituent metals of an attempted high entropy nanoparticle synthesis. In the top two patterns, diagnostic features include extra peaks, shoulders on peaks, and atypical peak shapes, as indicated.

broad peaks, low intensities, and the presence of closely spaced high-intensity peaks.<sup>46</sup>

The magenta-colored diffraction pattern at the top consists of a physical mixture of all the metals, each having a 5 nm grain size, to replicate complete phase segregation. Peak broadening does not appear to be uniform across the diffraction pattern because of how the peaks from the different phases (which have closely spaced lattice parameters) combine. Peak broadening appears to increase at higher  $2\theta$  values due to the increase in the separation of the overlapping constituent peaks. Peak asymmetry, the appearance of shoulders, and the presence of additional peaks are also evident. Such features in XRD patterns of nanoparticles claimed to be high entropy materials are common in the literature, highlighting the need for more careful analysis. Note that all of the XRD patterns in Figure 8 are shifted slightly relative to one another along the  $x$  axis, which is due to differences in composition and the extent of mixing. However, depending on the specific composition of a multimetal alloy, two-, three-, and four-metal alloys could possibly have the same peak positions as a five-metal alloy. Therefore, while the observation of a single-phase XRD pattern is important for claiming the formation of a high entropy material, it is not sufficient on its own.

## WHAT IS NEXT IN THE SYNTHESIS AND CHARACTERIZATION OF COLLOIDAL NANOPARTICLES OF HIGH ENTROPY MATERIALS?

The sections above briefly highlight current capabilities in synthesizing nanoparticles of colloidal high entropy materials as well as issues to consider in their formation, reactivity, and characterization. Now we turn to some current and emerging trends in the field as well as opportunities for the future. As many of the currently anticipated applications of high entropy nanoparticles are in heterogeneous catalysis, issues of bulk and surface composition as well as stability in reactive environments become increasingly important.<sup>73</sup> Also important for applications in heterogeneous catalysis are a fundamental understanding and quantitative description of strain modulation throughout the particle and surface as well as of the origin and implications of synergistic effects, including electronic, magnetic, and chemical properties. Given economic and environmental considerations, there is a push to minimize expensive and rare precious metals in catalytic materials, which motivates the development of high entropy nanoparticles that do not contain platinum group metals or that limit the amount that they incorporate. This requirement therefore motivates the development of reliable methods to make high entropy nanoparticles composed exclusively or predominantly of 3d transition metals and inexpensive s- and p-block metals. However, these are precisely the elements that have the highest reactivities, including being prone to oxidation and galvanic replacement. Careful synthesis and characterization are paramount here, as is consideration of the reaction pathways by which they form. Beyond the expanded incorporation of non-platinum-group metals, developing methods to synthesize nanoparticles of a broader scope of high entropy materials will also be important for advancing the field, including for areas beyond catalysis,<sup>8</sup> such as thermoelectric,<sup>74</sup> energy storage,<sup>75</sup> structural (anticorrosion, enhanced toughness),<sup>76</sup> magnetic,<sup>77</sup> electronic,<sup>78</sup> and optoelectronic materials.<sup>79</sup> As discussed in earlier sections, examples of high entropy sulfide, oxide, oxysulfide, and intermetallic nanoparticles exist, along with alloys, and progress is being made toward the synthesis of other classes of high entropy materials, including phosphides. Many more possibilities exist, though, and it will be exciting to see high entropy variants emerge across the broad scope of materials that are now mainstream in colloidal nanoparticle synthesis and applications.

Paramount to the opportunities mentioned in the preceding paragraph are the identification and understanding of the reaction pathways by which nanoparticles of high entropy materials are synthesized. These studies include mapping out the competing chemical reactivities that are inherent when so many reagents are simultaneously able to react independently and collectively as well as understanding how additives and adventitious elements help to trigger other reactions that ultimately lead to high entropy nanoparticle formation. Such efforts will lead to greater control over size, size uniformity, and shape as well as tunability of composition, structure, and surface chemistry. It will be interesting to learn for which systems the lessons already learned from the synthesis of single-metal and simpler two- and three-metal alloy and solid solution nanoparticles will be portable to high entropy materials. Understanding how and when existing knowledge translates to compositionally more complex nanoparticle

systems will simplify rational design efforts that target desired properties and applications. High entropy materials represent an emerging class of nanoparticles for which fundamental knowledge is still limited. Therefore, interrogating their chemical reactivity in different environments, such as those encountered during catalysis in applications such as fuel cells and batteries, is worthwhile and important both for the interiors and surfaces of the nanoparticles.

The challenges involved in characterization, discussed in the preceding section, also provide opportunities for expanding capabilities and gaining new knowledge about these complex nanomaterial systems. It is important to understand how elements are distributed within nanoparticles of high entropy materials as well as on their surfaces, especially for applications in catalysis. Coupled with where they are located in the interior versus on the surface are their chemical state and the chemical environment that they are in, including their oxidation states and coordination geometries. These features directly correlate to electronic structure, which defines their unique properties.<sup>80</sup> Unraveling the role of entropy in their formation and stabilization will also be useful for providing insights into how their synthesis can be approached as well as the range of environments in which they will be stable. Beyond aspects of characterization aimed at gaining new knowledge of high entropy nanoparticles, it is also important to promote and require minimum standards for routine characterization and analysis, as discussed in the preceding section, so that adequate and reliable information is available for any new systems that are reported.

All of the aspects of high entropy nanoparticle synthesis and characterization discussed in this Perspective can be viewed as prerequisites for rationally designing new systems with targeted features and for interrogating structure–property relationships in their emerging applications. With expanded knowledge of reaction pathways that can allow us to better target desired compositions, structures, morphologies, and surfaces, along with knowledge of chemical reactivity as it applies to high entropy nanoparticle systems, efforts to develop streamlined synthetic protocols will accelerate and become more efficient, pushing the field forward in new directions. Such capabilities will lead to nanoparticles of high entropy materials that are poised for useful applications and that will allow research to understand at a deep level how key aspects of their unique compositions influence properties, so that we can learn more about the emergence of synergistic effects in these compositionally complex systems. All of this is analogous to how our knowledge and capabilities involving nanoparticles of compositionally simpler systems have evolved in the past few decades, now with new challenges and opportunities that emerge from the unique compositional effects associated with mixing a large number of elements within nanoparticles. Finally, while this Perspective has focused primarily on experimental aspects of high entropy nanoparticle synthesis and characterization, advances in computational capabilities are important complements to experimental work. Computational studies have provided deep insights into the structures, properties, reactivity, formation, and stability of simpler nanoparticle systems, but handling the compositional and structural complexity of high entropy systems is challenging, but emerging.<sup>4,80,81</sup> Efforts to seamlessly integrate advanced and cutting-edge synthesis, characterization, and modeling, which is already underway, will greatly expand our understanding of these compositionally complex nanoscale materials, which in

turn has the potential to open new doors to previously unimagined properties and applications that leverage their unique features.

## AUTHOR INFORMATION

### Corresponding Author

**Raymond E. Schaak** – Department of Chemistry, Department of Chemical Engineering, and Materials Research Institute, The Pennsylvania State University, University Park, Pennsylvania 16802, United States; [orcid.org/0000-0002-7468-8181](https://orcid.org/0000-0002-7468-8181); Email: [res20@psu.edu](mailto:res20@psu.edu)

### Authors

**Gaurav R. Dey** – Department of Chemistry, The Pennsylvania State University, University Park, Pennsylvania 16802, United States; [orcid.org/0000-0001-8384-1048](https://orcid.org/0000-0001-8384-1048)

**Samuel S. Soliman** – Department of Chemistry, The Pennsylvania State University, University Park, Pennsylvania 16802, United States

**Connor R. McCormick** – Department of Chemistry, The Pennsylvania State University, University Park, Pennsylvania 16802, United States

**Charles H. Wood** – Department of Chemistry, The Pennsylvania State University, University Park, Pennsylvania 16802, United States

**Rowan R. Katzbaer** – Department of Chemistry, The Pennsylvania State University, University Park, Pennsylvania 16802, United States; [orcid.org/0000-0002-6028-2359](https://orcid.org/0000-0002-6028-2359)

Complete contact information is available at:

<https://pubs.acs.org/10.1021/acsnanoscienceau.3c00049>

### Notes

The authors declare no competing financial interest.

## ACKNOWLEDGMENTS

This work was supported by the U.S. National Science Foundation under Grant CHE-2203353. TEM and XRD data were acquired at the Materials Characterization Lab of the Penn State Materials Research Institute. The authors thank Sarah O'Boyle for helpful input on the design of the TOC graphic.

## REFERENCES

- (1) Yeh, J.-W.; Chen, S.-K.; Lin, S.-J.; Gan, J.-Y.; Chin, T.-S.; Shun, T.-T.; Tsau, C.-H.; Chang, S.-Y. Nanostructured High-Entropy Alloys with Multiple Principal Elements: Novel Alloy Design Concepts and Outcomes. *Adv. Eng. Mater.* **2004**, *6* (5), 299–303.
- (2) Yao, Y.; Huang, Z.; Xie, P.; Lacey, S. D.; Jacob, R. J.; Xie, H.; Chen, F.; Nie, A.; Pu, T.; Rehwoldt, M.; Yu, D.; Zachariah, M. R.; Wang, C.; Shahbazian-Yassar, R.; Li, J.; Hu, L. Carbothermal Shock Synthesis of High-Entropy-Alloy Nanoparticles. *Science* **2018**, *359* (6383), 1489–1494.
- (3) Löffler, T.; Savan, A.; Garzón-Manjón, A.; Meischein, M.; Scheu, C.; Ludwig, A.; Schuhmann, W. Toward a Paradigm Shift in Electrocatalysis Using Complex Solid Solution Nanoparticles. *ACS Energy Lett.* **2019**, *4* (5), 1206–1214.
- (4) Brahlek, M.; Gazda, M.; Keppens, V.; Mazza, A. R.; McCormack, S. J.; Mielewczyk-Gryn, A.; Musicco, B.; Page, K.; Rost, C. M.; Sinnott, S. B.; Toher, C.; Ward, T. Z.; Yamamoto, A. What Is in a Name: Defining “High Entropy” Oxides. *APL Mater.* **2022**, *10* (11), 110902.
- (5) Cantor, B.; Chang, I. T. H.; Knight, P.; Vincent, A. J. B. Microstructural Development in Equiatomic Multicomponent Alloys. *Mater. Sci. Eng., A* **2004**, *375*–377, 213–218.

- (6) Rost, C. M.; Sachet, E.; Borman, T.; Moballeghe, A.; Dickey, E. C.; Hou, D.; Jones, J. L.; Curtarolo, S.; Maria, J.-P. Entropy-Stabilized Oxides. *Nat. Commun.* **2015**, *6* (1), 8485.
- (7) Xin, Y.; Li, S.; Qian, Y.; Zhu, W.; Yuan, H.; Jiang, P.; Guo, R.; Wang, L. High-Entropy Alloys as a Platform for Catalysis: Progress, Challenges, and Opportunities. *ACS Catal.* **2020**, *10* (19), 11280–11306.
- (8) Sun, Y.; Dai, S. High-Entropy Materials for Catalysis: A New Frontier. *Sci. Adv.* **2021**, *7* (20), No. eabg1600.
- (9) Lv, Z. Y.; Liu, X. J.; Jia, B.; Wang, H.; Wu, Y.; Lu, Z. P. Development of a Novel High-Entropy Alloy with Eminent Efficiency of Degrading Azo Dye Solutions. *Sci. Rep.* **2016**, *6* (1), 34213.
- (10) Tsai, C.-F.; Wu, P.-W.; Lin, P.; Chao, C.-G.; Yeh, K.-Y. Sputter Deposition of Multi-Element Nanoparticles as Electrocatalysts for Methanol Oxidation. *Jpn. J. Appl. Phys.* **2008**, *47* (7), 5755–5761.
- (11) Löffler, T.; Meyer, H.; Savan, A.; Wilde, P.; Garzón Manjón, A.; Chen, Y.; Ventosa, E.; Scheu, C.; Ludwig, A.; Schuhmann, W. Discovery of a Multinary Noble Metal-Free Oxygen Reduction Catalyst. *Adv. Energy Mater.* **2018**, *8* (34), 1802269.
- (12) Waag, F.; Li, Y.; Zieffuß, A. R.; Bertin, E.; Kamp, M.; Duppel, V.; Marzun, G.; Kienle, L.; Barcikowski, S.; Gökce, B. Kinetically-Controlled Laser-Synthesis of Colloidal High-Entropy Alloy Nanoparticles. *RSC Adv.* **2019**, *9* (32), 18547–18558.
- (13) Liu, M.; Zhang, Z.; Okejiri, F.; Yang, S.; Zhou, S.; Dai, S. Entropy-Maximized Synthesis of Multimetallic Nanoparticle Catalysts via a Ultrasonication-Assisted Wet Chemistry Method under Ambient Conditions. *Adv. Mater. Interfaces* **2019**, *6* (7), 1900015.
- (14) Yang, Y.; Song, B.; Ke, X.; Xu, F.; Bozhilov, K. N.; Hu, L.; Shahbazian-Yassar, R.; Zachariah, M. R. Aerosol Synthesis of High Entropy Alloy Nanoparticles. *Langmuir* **2020**, *36* (8), 1985–1992.
- (15) Phakatkar, A. H.; Saray, M. T.; Rasul, M. G.; Sorokina, L. V.; Ritter, T. G.; Shokuhfar, T.; Shahbazian-Yassar, R. Ultrafast Synthesis of High Entropy Oxide Nanoparticles by Flame Spray Pyrolysis. *Langmuir* **2021**, *37* (30), 9059–9068.
- (16) Qiao, H.; Saray, M. T.; Wang, X.; Xu, S.; Chen, G.; Huang, Z.; Chen, C.; Zhong, G.; Dong, Q.; Hong, M.; Xie, H.; Shahbazian-Yassar, R.; Hu, L. Scalable Synthesis of High Entropy Alloy Nanoparticles by Microwave Heating. *ACS Nano* **2021**, *15* (9), 14928–14937.
- (17) Yao, Y.; Huang, Z.; Hughes, L. A.; Gao, J.; Li, T.; Morris, D.; Zeltmann, S. E.; Savitzky, B. H.; Ophus, C.; Finrock, Y. Z.; Dong, Q.; Jiao, M.; Mao, Y.; Chi, M.; Zhang, P.; Li, J.; Minor, A. M.; Shahbazian-Yassar, R.; Hu, L. Extreme Mixing in Nanoscale Transition Metal Alloys. *Matter* **2021**, *4* (7), 2340–2353.
- (18) Cui, M.; Yang, C.; Hwang, S.; Yang, M.; Overa, S.; Dong, Q.; Yao, Y.; Brozena, A. H.; Cullen, D. A.; Chi, M.; Blum, T. F.; Morris, D.; Finrock, Z.; Wang, X.; Zhang, P.; Goncharov, V. G.; Guo, X.; Luo, J.; Mo, Y.; Jiao, F.; Hu, L. Multi-Principal Elemental Intermetallic Nanoparticles Synthesized via a Disorder-to-Order Transition. *Sci. Adv.* **2022**, *8* (4), No. eabm4322.
- (19) Li, T.; Yao, Y.; Huang, Z.; Xie, P.; Liu, Z.; Yang, M.; Gao, J.; Zeng, K.; Brozena, A. H.; Pastel, G.; Jiao, M.; Dong, Q.; Dai, J.; Li, S.; Zong, H.; Chi, M.; Luo, J.; Mo, Y.; Wang, G.; Wang, C.; Shahbazian-Yassar, R.; Hu, L. Denary Oxide Nanoparticles as Highly Stable Catalysts for Methane Combustion. *Nat. Catal.* **2021**, *4* (1), 62–70.
- (20) Niu, B.; Zhang, F.; Ping, H.; Li, N.; Zhou, J.; Lei, L.; Xie, J.; Zhang, J.; Wang, W.; Fu, Z. Sol-Gel Autocombustion Synthesis of Nanocrystalline High-Entropy Alloys. *Sci. Rep.* **2017**, *7* (1), 3421.
- (21) Minamihara, H.; Kusada, K.; Wu, D.; Yamamoto, T.; Toriyama, T.; Matsumura, S.; Kumara, L. S. R.; Ohara, K.; Sakata, O.; Kawaguchi, S.; Kubota, Y.; Kitagawa, H. Continuously-Flow Reactor Synthesis for Homogeneous 1 nm-Sized Extremely Small High-Entropy Alloy Nanoparticles. *J. Am. Chem. Soc.* **2022**, *144* (26), 11525–11529.
- (22) Kwon, H. J.; Shin, K.; Soh, M.; Chang, H.; Kim, J.; Lee, J.; Ko, G.; Kim, B. H.; Kim, D.; Hyeon, T. Large-Scale Synthesis and Medical Applications of Uniform-Sized Metal Oxide Nanoparticles. *Adv. Mater.* **2018**, *30* (42), 1704290.
- (23) Saldanha, P. L.; Lesnyak, V.; Manna, L. Large Scale Syntheses of Colloidal Nanomaterials. *Nano Today* **2017**, *12*, 46–63.
- (24) Shi, Y.; Lyu, Z.; Zhao, M.; Chen, R.; Nguyen, Q. N.; Xia, Y. Noble-Metal Nanocrystals with Controlled Shapes for Catalytic and Electrocatalytic Applications. *Chem. Rev.* **2021**, *121* (2), 649–735.
- (25) Xia, Y.; Xiong, Y.; Lim, B.; Skrabalak, S. E. Shape-Controlled Synthesis of Metal Nanocrystals: Simple Chemistry Meets Complex Physics? *Angew. Chem., Int. Ed.* **2009**, *48* (1), 60–103.
- (26) Wu, D.; Kusada, K.; Yamamoto, T.; Toriyama, T.; Matsumura, S.; Kawaguchi, S.; Kubota, Y.; Kitagawa, H. Platinum-Group-Metal High-Entropy-Alloy Nanoparticles. *J. Am. Chem. Soc.* **2020**, *142* (32), 13833–13838.
- (27) Dey, G. R.; McCormick, C. R.; Soliman, S. S.; Darling, A. J.; Schaak, R. E. Chemical Insights into the Formation of Colloidal High Entropy Alloy Nanoparticles. *ACS Nano* **2023**, *17* (6), 5943–5955.
- (28) Chen, W.; Luo, S.; Sun, M.; Wu, X.; Zhou, Y.; Liao, Y.; Tang, M.; Fan, X.; Huang, B.; Quan, Z. High-Entropy Intermetallic PtRhBiSnSb Nanoplates for Highly Efficient Alcohol Oxidation Electrocatalysis. *Adv. Mater.* **2022**, *34* (43), 2206276.
- (29) Soliman, S. S.; Dey, G. R.; McCormick, C. R.; Schaak, R. E. Temporal Evolution of Morphology, Composition, and Structure in the Formation of Colloidal High-Entropy Intermetallic Nanoparticles. *ACS Nano* **2023**, *17* (16), 16147–16159.
- (30) Zhan, C.; Bu, L.; Sun, H.; Huang, X.; Zhu, Z.; Yang, T.; Ma, H.; Li, L.; Wang, Y.; Geng, H.; Wang, W.; Zhu, H.; Pao, C.; Shao, Q.; Yang, Z.; Liu, W.; Xie, Z.; Huang, X. Medium/High-Entropy Amalgamated Core/Shell Nanoplate Achieves Efficient Formic Acid Catalysis for Direct Formic Acid Fuel Cell. *Angew. Chem., Int. Ed.* **2023**, *62* (3), No. e202213783.
- (31) Nakamura, M.; Wu, D.; Mukoyoshi, M.; Kusada, K.; Toriyama, T.; Yamamoto, T.; Matsumura, S.; Murakami, Y.; Kawaguchi, S.; Kubota, Y.; Kitagawa, H. B2-Structured Indium-Platinum Group Metal High-Entropy Intermetallic Nanoparticles. *Chem. Commun.* **2023**, *59* (62), 9485–9488.
- (32) McCormick, C. R.; Schaak, R. E. Simultaneous Multication Exchange Pathway to High-Entropy Metal Sulfide Nanoparticles. *J. Am. Chem. Soc.* **2021**, *143* (2), 1017–1023.
- (33) Li, F.; Ma, Y.; Wu, H.; Zhai, Q.; Zhao, J.; Ji, H.; Tang, S.; Meng, X. Sub-3-nm High-Entropy Metal Sulfide Nanoparticles with Synergistic Effects as Promising Electrocatalysts for Enhanced Oxygen Evolution Reaction. *J. Phys. Chem. C* **2022**, *126* (43), 18323–18332.
- (34) Moradi, M.; Hasanvandian, F.; Bahadoran, A.; Shokri, A.; Zerangnasrabad, S.; Kakavandi, B. New High-Entropy Transition-Metal Sulfide Nanoparticles for Electrochemical Oxygen Evolution Reaction. *Electrochim. Acta* **2022**, *436*, 141444.
- (35) Nguyen, T. X.; Su, Y.; Lin, C.; Ting, J. Self-Reconstruction of Sulfate-Containing High Entropy Sulfide for Exceptionally High-Performance Oxygen Evolution Reaction Electrocatalyst. *Adv. Funct. Mater.* **2021**, *31* (48), 2106229.
- (36) Xu, Y.; Wang, L.; Shi, Z.; Su, N.; Li, C.; Huang, Y.; Huang, N.; Deng, Y.; Li, H.; Ma, T.; Kong, X. Y.; Lin, W.; Zhou, Y.; Ye, L. Peroxide-Mediated Selective Conversion of Biomass Polysaccharides over High Entropy Sulfides via Solar Energy Catalysis. *Energy Environ. Sci.* **2023**, *16* (4), 1531–1539.
- (37) Zhong, Z.; Fu, H.; Wang, S.; Duan, Y.; Wang, Q.; Yan, C.; Du, Y. A Universal Synthesis Strategy for Lanthanide Sulfide Nanocrystals with Efficient Photocatalytic Hydrogen Production. *Small* **2023**, *19* (33), 2301392.
- (38) Shi, Y.; Xu, Q.; Tian, Z.; Liu, G.; Ma, C.; Zheng, W. Ionic Liquid-Hydroxide-Mediated Low-Temperature Synthesis of High-Entropy Perovskite Oxide Nanoparticles. *Nanoscale* **2022**, *14* (21), 7817–7827.
- (39) Wang, G.; Qin, J.; Feng, Y.; Feng, B.; Yang, S.; Wang, Z.; Zhao, Y.; Wei, J. Sol-Gel Synthesis of Spherical Mesoporous High-Entropy Oxides. *ACS Appl. Mater. Interfaces* **2020**, *12* (40), 45155–45164.
- (40) Wang, D.; Liu, Z.; Du, S.; Zhang, Y.; Li, H.; Xiao, Z.; Chen, W.; Chen, R.; Wang, Y.; Zou, Y.; Wang, S. Low-Temperature Synthesis of Small-Sized High-Entropy Oxides for Water Oxidation. *J. Mater. Chem. A* **2019**, *7* (42), 24211–24216.



- (41) Li, F.; Sun, S.-K.; Chen, Y.; Naka, T.; Hashishin, T.; Maruyama, J.; Abe, H. Bottom-up Synthesis of 2D Layered High-Entropy Transition Metal Hydroxides. *Nanoscale Adv.* **2022**, *4* (11), 2468–2478.
- (42) Ward-O'Brien, B.; McNaughton, P. D.; Cai, R.; Chattopadhyay, A.; Flitcroft, J. M.; Smith, C. T.; Binks, D. J.; Skelton, J. M.; Haigh, S. J.; Lewis, D. J. Quantum Confined High-Entropy Lanthanide Oxysulfide Colloidal Nanocrystals. *Nano Lett.* **2022**, *22* (20), 8045–8051.
- (43) Broge, N. L. N.; Bondesgaard, M.; Søndergaard-Pedersen, F.; Roelsgaard, M.; Iversen, B. B. Autocatalytic Formation of High-Entropy Alloy Nanoparticles. *Angew. Chem., Int. Ed.* **2020**, *132* (49), 22104–22108.
- (44) Li, H.; Han, Y.; Zhao, H.; Qi, W.; Zhang, D.; Yu, Y.; Cai, W.; Li, S.; Lai, J.; Huang, B.; Wang, L. Fast Site-to-Site Electron Transfer of High-Entropy Alloy Nanocatalyst Driving Redox Electrocatalysis. *Nat. Commun.* **2020**, *11* (1), 5437.
- (45) Chen, Y.; Zhan, X.; Bueno, S. L. A.; Shafei, I. H.; Ashberry, H. M.; Chatterjee, K.; Xu, L.; Tang, Y.; Skrabalak, S. E. Synthesis of Monodisperse High Entropy Alloy Nanocatalysts from Core@shell Nanoparticles. *Nanoscale Horiz.* **2021**, *6* (3), 231–237.
- (46) Bueno, S. L. A.; Leonardi, A.; Kar, N.; Chatterjee, K.; Zhan, X.; Chen, C.; Wang, Z.; Engel, M.; Fung, V.; Skrabalak, S. E. Quinary, Senary, and Septenary High Entropy Alloy Nanoparticle Catalysts from Core@Shell Nanoparticles and the Significance of Intraparticle Heterogeneity. *ACS Nano* **2022**, *16* (11), 18873–18885.
- (47) Kar, N.; McCoy, M.; Wolfe, J.; Bueno, S. L. A.; Shafei, I. H.; Skrabalak, S. E. Retrosynthetic Design of Core-Shell Nanoparticles for Thermal Conversion to Monodisperse High-Entropy Alloy Nanoparticles. *Nat. Synth.* **2023**, DOI: 10.1038/s44160-023-00409-0.
- (48) Antolini, E. Alloy vs. Intermetallic Compounds: Effect of the Ordering on the Electrocatalytic Activity for Oxygen Reduction and the Stability of Low Temperature Fuel Cell Catalysts. *Appl. Catal., B* **2017**, *217*, 201–213.
- (49) Gamler, J. T. L.; Ashberry, H. M.; Skrabalak, S. E.; Koczkur, K. M. Random Alloyed versus Intermetallic Nanoparticles: A Comparison of Electrocatalytic Performance. *Adv. Mater.* **2018**, *30* (40), 1801563.
- (50) Su'a, T.; Poli, M. N.; Brock, S. L. Homogeneous Nanoparticles of Multimetallic Phosphides via Precursor Tuning: Ternary and Quaternary  $M_2P$  Phases ( $M = Fe, Co, Ni$ ). *ACS Nanosci. Au* **2022**, *2* (6), 503–519.
- (51) Niederberger, M.; Garnweitner, G. Organic Reaction Pathways in the Nonaqueous Synthesis of Metal Oxide Nanoparticles. *Chem. - Eur. J.* **2006**, *12* (28), 7282–7302.
- (52) Liu, Y.-H.; Hsieh, C.-J.; Hsu, L.-C.; Lin, K.-H.; Hsiao, Y.-C.; Chi, C.-C.; Lin, J.-T.; Chang, C.-W.; Lin, S.-C.; Wu, C.-Y.; Gao, J.-Q.; Pao, C.-W.; Chang, Y.-M.; Lu, M.-Y.; Zhou, S.; Yang, T.-H. Toward Controllable and Predictable Synthesis of High-Entropy Alloy Nanocrystals. *Sci. Adv.* **2023**, *9* (19), No. eadf9931.
- (53) Chen, Z.; Wen, J.; Wang, C.; Kang, X. Convex Cube-Shaped  $Pt_{34}Fe_3Ni_{20}Cu_3Mo_9$  Ru High Entropy Alloy Catalysts toward High-Performance Multifunctional Electrocatalysis. *Small* **2022**, *18* (45), 2204255.
- (54) Lao, X.; Liao, X.; Chen, C.; Wang, J.; Yang, L.; Li, Z.; Ma, J.; Fu, A.; Gao, H.; Guo, P. Pd-Enriched-Core/Pt-Enriched-Shell High-Entropy Alloy with Face-Centred Cubic Structure for  $C_1$  and  $C_2$  Alcohol Oxidation. *Angew. Chem., Int. Ed.* **2023**, *62* (31), No. e202304510.
- (55) Zhang, D.; Shi, Y.; Zhao, H.; Qi, W.; Chen, X.; Zhan, T.; Li, S.; Yang, B.; Sun, M.; Lai, J.; Huang, B.; Wang, L. The Facile Oil-Phase Synthesis of a Multi-Site Synergistic High-Entropy Alloy to Promote the Alkaline Hydrogen Evolution Reaction. *J. Mater. Chem. A* **2021**, *9* (2), 889–893.
- (56) Zhang, D.; Zhao, H.; Wu, X.; Deng, Y.; Wang, Z.; Han, Y.; Li, H.; Shi, Y.; Chen, X.; Li, S.; Lai, J.; Huang, B.; Wang, L. Multi-Site Electrocatalysts Boost pH-Universal Nitrogen Reduction by High-Entropy Alloys. *Adv. Funct. Mater.* **2021**, *31* (9), 2006939.
- (57) Fu, X.; Zhang, J.; Zhan, S.; Xia, F.; Wang, C.; Ma, D.; Yue, Q.; Wu, J.; Kang, Y. High-Entropy Alloy Nanosheets for Fine-Tuning Hydrogen Evolution. *ACS Catal.* **2022**, *12* (19), 11955–11959.
- (58) Zhan, C.; Xu, Y.; Bu, L.; Zhu, H.; Feng, Y.; Yang, T.; Zhang, Y.; Yang, Z.; Huang, B.; Shao, Q.; Huang, X. Subnanometer High-Entropy Alloy Nanowires Enable Remarkable Hydrogen Oxidation Catalysis. *Nat. Commun.* **2021**, *12* (1), 6261.
- (59) Sun, Y.; Zhang, W.; Zhang, Q.; Li, Y.; Gu, L.; Guo, S. A General Approach to High-Entropy Metallic Nanowire Electrocatalysts. *Matter* **2023**, *6* (1), 193–205.
- (60) Singh, M. P.; Srivastava, C. Synthesis and Electron Microscopy of High Entropy Alloy Nanoparticles. *Mater. Lett.* **2015**, *160*, 419–422.
- (61) Tao, L.; Sun, M.; Zhou, Y.; Luo, M.; Lv, F.; Li, M.; Zhang, Q.; Gu, L.; Huang, B.; Guo, S. A General Synthetic Method for High-Entropy Alloy Subnanometer Ribbons. *J. Am. Chem. Soc.* **2022**, *144* (23), 10582–10590.
- (62) Williamson, E. M.; Sun, Z.; Mora-Tamez, L.; Brutchey, R. L. Design of Experiments for Nanocrystal Syntheses: A How-To Guide for Proper Implementation. *Chem. Mater.* **2022**, *34* (22), 9823–9835.
- (63) Williamson, E. M.; Brutchey, R. L. Using Data-Driven Learning to Predict and Control the Outcomes of Inorganic Materials Synthesis. *Inorg. Chem.* **2023**, *62* (40), 16251–16262.
- (64) Mints, V. A.; Pedersen, J. K.; Bagger, A.; Quinson, J.; Anker, A. S.; Jensen, K. M. Ø.; Rossmeisl, J.; Arenz, M. Exploring the Composition Space of High-Entropy Alloy Nanoparticles for the Electrocatalytic  $H_2$  /CO Oxidation with Bayesian Optimization. *ACS Catal.* **2022**, *12* (18), 11263–11271.
- (65) Guisbiers, G.; Mendoza-Cruz, R.; Bazán-Díaz, L.; Velázquez-Salazar, J. J.; Mendoza-Perez, R.; Robledo-Torres, J. A.; Rodríguez-Lopez, J.-L.; Montejano-Carrizales, J. M.; Whetten, R. L.; José-Yacamán, M. Electrum, the Gold-Silver Alloy, from the Bulk Scale to the Nanoscale: Synthesis, Properties, and Segregation Rules. *ACS Nano* **2016**, *10* (1), 188–198.
- (66) Zakhtser, A.; Naitabdi, A.; Benbalagh, R.; Rochet, F.; Salzemann, C.; Petit, C.; Giorgio, S. Chemical Evolution of Pt-Zn Nanoalloys Dressed in Oleylamine. *ACS Nano* **2021**, *15* (3), 4018–4033.
- (67) Liao, H.; Fisher, A.; Xu, Z. J. Surface Segregation in Bimetallic Nanoparticles: A Critical Issue in Electrocatalyst Engineering. *Small* **2015**, *11* (27), 3221–3246.
- (68) Song, B.; Yang, Y.; Yang, T. T.; He, K.; Hu, X.; Yuan, Y.; Dravid, V. P.; Zachariah, M. R.; Saidi, W. A.; Liu, Y.; Shahbazian-Yassar, R. Revealing High-Temperature Reduction Dynamics of High-Entropy Alloy Nanoparticles via *In Situ* Transmission Electron Microscopy. *Nano Lett.* **2021**, *21* (4), 1742–1748.
- (69) Feng, G.; Ning, F.; Song, J.; Shang, H.; Zhang, K.; Ding, Z.; Gao, P.; Chu, W.; Xia, D. Sub-2 nm Ultrasmall High-Entropy Alloy Nanoparticles for Extremely Superior Electrocatalytic Hydrogen Evolution. *J. Am. Chem. Soc.* **2021**, *143* (41), 17117–17127.
- (70) Kusada, K.; Wu, D.; Kitagawa, H. New Aspects of Platinum Group Metal-Based Solid-Solution Alloy Nanoparticles: Binary to High-Entropy Alloys. *Chem. - Eur. J.* **2020**, *26* (23), 5105–5130.
- (71) Holder, C. F.; Schaak, R. E. Tutorial on Powder X-ray Diffraction for Characterizing Nanoscale Materials. *ACS Nano* **2019**, *13* (7), 7359–7365.
- (72) Jain, A.; Ong, S. P.; Hautier, G.; Chen, W.; Richards, W. D.; Dacek, S.; Cholia, S.; Gunter, D.; Skinner, D.; Ceder, G.; Persson, K. A. Commentary: The Materials Project: A Materials Genome Approach to Accelerating Materials Innovation. *APL Mater.* **2013**, *1* (1), 011002.
- (73) Maulana, A. L.; Chen, P.-C.; Shi, Z.; Yang, Y.; Lizandara-Pueyo, C.; Seeler, F.; Abruña, H. D.; Muller, D.; Schierle-Arndt, K.; Yang, P. Understanding the Structural Evolution of IrFeCoNiCu High-Entropy Alloy Nanoparticles under the Acidic Oxygen Evolution Reaction. *Nano Lett.* **2023**, *23* (14), 6637–6644.
- (74) Wang, X.; Yao, H.; Zhang, Z.; Li, X.; Chen, C.; Yin, L.; Hu, K.; Yan, Y.; Li, Z.; Yu, B.; Cao, F.; Liu, X.; Lin, X.; Zhang, Q. Enhanced Thermoelectric Performance in High Entropy Alloys

$\text{Sn}_{0.25}\text{Pb}_{0.25}\text{Mn}_{0.25}\text{Ge}_{0.25}\text{Te}$ . *ACS Appl. Mater. Interfaces* **2021**, *13* (16), 18638–18647.

(75) Amiri, A.; Shahbazian-Yassar, R. Recent Progress of High-Entropy Materials for Energy Storage and Conversion. *J. Mater. Chem. A* **2021**, *9* (2), 782–823.

(76) Wu, P.; Gan, K.; Yan, D.; Fu, Z.; Li, Z. A Non-Equiatomic FeNiCoCr High-Entropy Alloy with Excellent Anti-Corrosion Performance and Strength-Ductility Synergy. *Corros. Sci.* **2021**, *183*, 109341.

(77) Kumari, P.; Gupta, A. K.; Mishra, R. K.; Ahmad, M. S.; Shahi, R. R. A Comprehensive Review: Recent Progress on Magnetic High Entropy Alloys and Oxides. *J. Magn. Magn. Mater.* **2022**, *554*, 169142.

(78) Nemani, S. K.; Torkamanzadeh, M.; Wyatt, B. C.; Presser, V.; Anasori, B. Functional Two-Dimensional High-Entropy Materials. *Commun. Mater.* **2023**, *4* (1), 16.

(79) Corey, Z. J.; Lu, P.; Zhang, G.; Sharma, Y.; Rutherford, B. X.; Dhole, S.; Roy, P.; Wang, Z.; Wu, Y.; Wang, H.; Chen, A.; Jia, Q. Structural and Optical Properties of High Entropy (La, Lu, Y, Gd, Ce)AlO<sub>3</sub> Perovskite Thin Films. *Adv. Sci.* **2022**, *9* (29), 2202671.

(80) Wu, D.; Kusada, K.; Yamamoto, T.; Toriyama, T.; Matsumura, S.; Gueye, I.; Seo, O.; Kim, J.; Hiroi, S.; Sakata, O.; Kawaguchi, S.; Kubota, Y.; Kitagawa, H. On the Electronic Structure and Hydrogen Evolution Reaction Activity of Platinum Group Metal-Based High-Entropy-Alloy Nanoparticles. *Chem. Sci.* **2020**, *11* (47), 12731–12736.

(81) Wan, X.; Li, Z.; Yu, W.; Wang, A.; Ke, X.; Guo, H.; Su, J.; Li, L.; Gui, Q.; Zhao, S.; Robertson, J.; Zhang, Z.; Guo, Y. Machine Learning Paves the Way for High Entropy Compounds Exploration: Challenges, Progress, and Outlook. *Adv. Mater.* **2023**, DOI: 10.1002/adma.202305192.